BULETINUL INSTITUTULUI POLITEHNIC DIN IAŞI

Tomul LIV (LVIII)

Fasc. 2

HIDROTEHNICĂ

2008

BULETINUL INSTITUTULUI POLITEHNIC DIN IAŞI
PUBLISHED BY
TECHNICAL UNIVERSITY „GHEORGHE ASACHI" OF IASI
Editorial Office: Bd. D. Mangeron 63, 700050, Iaşi, ROMANIA
Tel. 40-232-278683; Fax: 40-232 237666; e-mail: polytech@mail.tuiasi.ro

BULETINUL INSTITUTULUI POLITEHNIC DIN IAŞI
BULLETIN OF THE POLYTECHNIC INSTITUTE OF JASSY
Tomul LIV (LVIII), Fasc. 2 2008

HIDROTEHNICĂ

CONTENTS

Pp.

BULETINUL INSTITUTULUI POLITEHNIC DIN IAŞI
BULLETIN OF THE POLYTECHNIC INSTITUTE OF JASSY
Tomul LIV (LVIII), Fasc. 2 2008

HIDROTEHNICĂ

SUMAR

BULETINUL INSTITUTULUI POLITEHNIC DIN IAŞI
Publicat de
Universitatea Tehnică „Gheorghe Asachi" din Iaşi
Tomul LIV (LVIII), Fasc. 2, 2008
Secţia
HIDROTEHNICĂ

THE EVOLUTION OF HYDROLOGICAL PARAMETERS IN REPRESENTATIVE BASIN TINOASA-CIUREA , DISTRICT IASI

BY

FLORIAN STĂTESCU and CLAUDIU PRICOP

This paper presents results and evaluations covering a longer period of time, based on data obtained from the observation and measurements of various parameters recorded in the Tinoasa – Ciurea representative basin.

1. Introduction

The representative basins definition: those research units that on a 1:1 scale model series, in natural conditions, in which an intensive programme of hydrometeorologic observations is being carried out, provide the possibility to determine the elements required to establish the principles obtained in the experimental stations.

In the representative basins, there is the possibility to follow up the leakage processes, starting from particular cases to general ones, an opportunity that can lead to irrefutable conclusions regarding the influence that various factors have on the leakage [1].

By influencing these units and via the research carried out there, there is a possibility to find answers to many hydrological issues, using a limited number of observation points and measurements.

The obtained results during this research are ultimately used to check the existent graphical or mathematical relations related to the leakage, as well as to establish their components (the hydrological parameters) for their subsequent practical application [2,..,4].

Given the importance of representative basins in the research of leakage forming processes on small rivers, a series of criteria were taken into consideration for their selection, including:

a) the diversity of physical-geographical conditions in the basin (relief forms, slopes, geology, geomorphology, soils and vegetation) and varied subbasin general forms;

Fig.1. Location of Ciurea Tinoasa basin, on a scale of 1:25 000

b) the representative basin must be typical for vast territories in the country;

c) the existence inside the representative basin of subbasins which allow for the investigation of factors which generate the leakage on experimental areas and very small basin areas;

d) a high homogeneity of the subbasin conditions so as not to make many corrections to the leakage parameters;

e) the degree of river usage in the representative basin should be as low as possible, so that it does not significantly impact the hydrological regime;

f) the existence of a meteorology station inside or near the representative basin, to provide climatic data covering and which – correlated

with the data obtained for short periods of time – would eventually help determinate the hydrological parameters.

The representative basins have been located in various natural conditions, to underline the role that the most important factors have on leakage formation, e.g. the receptive basin's area, medium altitude, medium slope and physical-geographical characteristics such as: geology, relief, climate, soil, vegetation.

2. Material and Methods

Tinoasa-Ciurea representative basin was established in 1969 and it is situated in the hydrographic basin of Bahlui river. The closest locality to the closing section is Ciurea, Iasi County.

The morphometric data and forestation coefficients are presented in Table 1:

Table 1

Characteristic Data of Tinoasa-Ciurea Basin

Basin name	Basin area [Km²]	Profile altitude [m]	Maximum altitude [m]	Medium altitude [m]	Streambed length [Km]	Streambed slope ‰	Medium basin slope [‰]	Forestation coefficient %
Rusu	1,54	123,50	390	280	2,13	110,3	152	87,9
Bolovani	0,50	124,28	335	250,4	1,18	102,3	153	33,4
Ciurel	0,17	122,55	192	158	0,48	140,4	157	0,0
Humaria	1,60	120.06	410	270	2,14	111,0	170	100
Tinoasa	4,17	118,80	410	272	2,32	103,9	159	77,6

Data regarding the physical-geographical characteristics of the Tinoasa-Ciurea representative basin are

a) geology: bedrock and clays are predominant, rubles, sands and loess are also found

b) relief: downy, situated at the border between the Central Moldavian Plateau and the Moldavian Plain, with heights between 410 and 125 meters, and slops between 125 ‰ and 170 ‰;

c) climate: continental sometimes excessive continental, hills with predominant north-west circulation, with multiyear medium precipitations between 595-600 mm and multiyear medium air temperatures of 9ºC;
d) soil: brown and forest brown hectic soils, and also pseudo rendzine;
e) vegetation: deciduous forests are predominant; there are also meadows and pastures.

In the Tinoasa-Ciurea representative basin, a complex program of observation and hydrometeorology measurements is currently carried out.

On the meteorology platform, observation and measurements at standard hours are taken: liquid and solid precipitations, air temperature (ordinary, minimum, maximum), air humidity, wind direction and speed, evaporation at soil surface.

Tinoasa-Ciurea representative basin has five sections on Rusu, Bolovani, Ciurel, Humaria and Tinoasa (closing section) rivers, where the levels, liquid flow capacity and suspension silts are registered.

Tinoasa-Ciurea representative basin has leakage holdings (including a free leakage holding and two concrete platforms), on which leakage capacity measurements of slope leakage are performed. In addition, the Tinoasa-Ciurea representative basin has a drilling alignment which is used for piezometric observations and measurements.

The obtained data in the Tinoasa-Ciurea representative basin, based on the observations and measurements carried out during the last 15 years (1992-2007), has been used for analysis and characterization of this period, and also for identification of new evolution trends of main climatic parameters.

The idea for this analysis came due to the climatic changes recorded in Romania.

3. Results and discussions

The conclusion is that the observations and measurements carried out in Romania highlight a series of signals pointing to future climatic changes, many of them having similar trends with world changes.

The changes include the evolution of main climatic parameters (temperature, precipitation, moisture, flood regime), season sequence and the existence of phenomena and desertification trends.

From the registered data, some aspects stand out, including

a) the medium air temperature at field surface is increasing;
b) a slight increase of the medium annual temperature and a precipitation decrease;
c) extreme temperatures have been recorded;

The most important modifications of the hydrological regime, doubled by their consequences, include:

a) the increase of evaporation in the summer season due to the air temperature increase;
b) the extension of small water periods and the reduction of minimum flows due to increased evaporation and decreased precipitations in summer;
c) the earlier burst of nival floods and the reduction of mixed floods (snow-rain) in spring, due to the desynchronization between the melting snow layer and spring rains.

Using the data obtained in the last 15 years in the Ciurea -Tinoasa representative basin, monthly, annual and multiyear medium flows for the five sections (Rusu, Bolovani, Ciurel, Humăria and Tinoasa) were determined as well as the medium number of days per month, year and multiyear when the leakage on every river was generated [5],[6].

By comparing the multiyear medium values with the ones recorded in 2007, we developed an evaluation of leakage for the above mentioned period.

The graphical presentation of the evaluation from January to September 2007 versus the multiyear values is show in Fig. 2

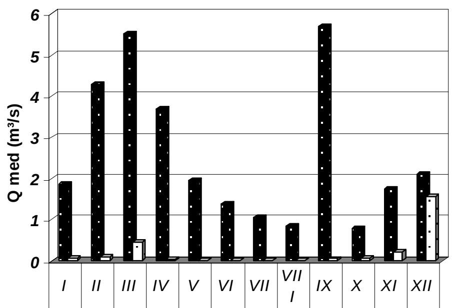

	I	II	III	IV	V	VI	VII	VIII	IX	X	XI	XII
Q med multiyear	1.9	4.3	5.5	3.7	1.9	1.4	1	0.9	5.7	0.8	1.7	2.1
Q med 2007	0.1	0.1	0.4	0	0	0	0	0	0	0.1	0.2	1.6

Fig. 2 Bolovani River; the variation of the average mounthly and multyear flows

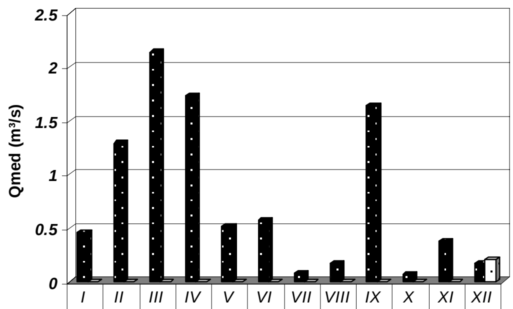

	I	II	III	IV	V	VI	VII	VIII	IX	X	XI	XII
Q med multiyear	0.46	1.29	2.14	1.73	0.52	0.57	0.08	0.17	1.64	0.07	0.37	0.17
Q med 2007	0	0	0	0	0	0	0	0	0	0	0	0.2

Fig. 3 Ciurel river; the variation of the average mounthly and multyear flows

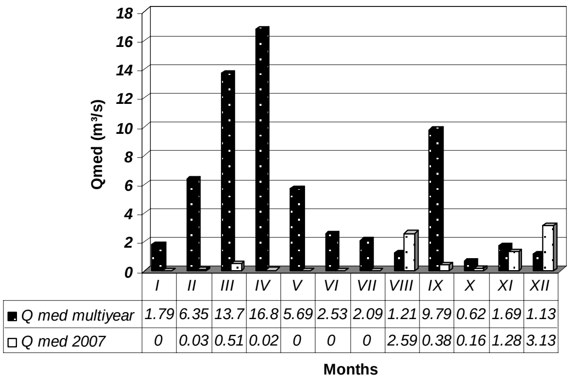

Fig. 4 .Humaria river the variation of the average mounthly and multyear flows

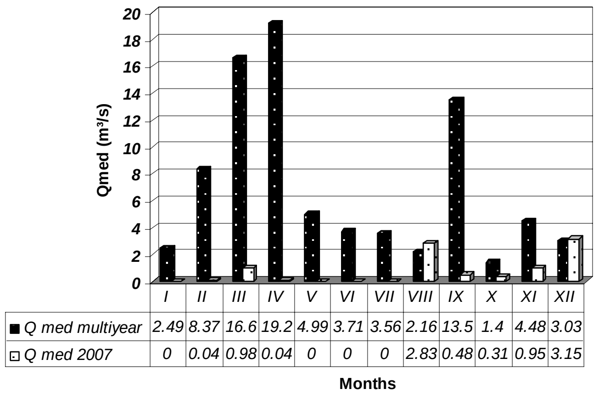

Fig. 5 Rusu river the variation of the average mounthly and multyear flows

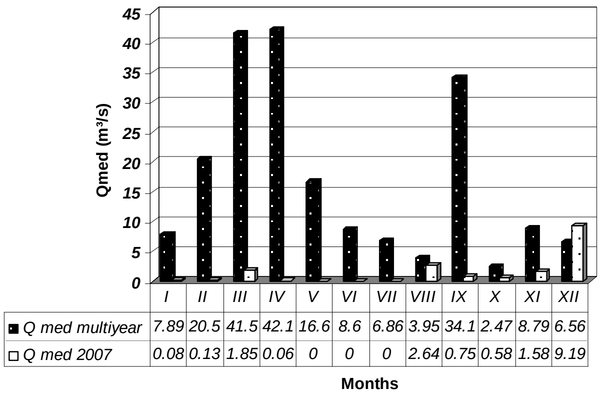

Fig. 6 .Tinoasa river; the variation of the average mounthly and multyear flows

4. Conclusions

The analysis of the parameters measured in the Tionoasa – Ciurea representative basin showed that the year 2007 was characterized by a liquid flow with values significantly lower than the multiyear medium values, with few days when the water flew in the five sections, and 90 consecutive dry days recorded.

The leakage was a consequence of both the thermal regime with air medium temperatures higher than the multiyear values, and also of the deficitary pluviometric regime caused by a period without substantial precipitations at the end of 2006.

Received, May 7, 2008

Technical University "Gh. Asachi", Iassy,
Department Hidroamelioration and Environment Protection
[x]National Administration of Romanian Water, Directorate Prut Iassy

REFERENCES

1. B ă l o i V., *Amenajarea bazinelor hidrografice şi a cursurilor de apă*, Ed. Ceres, Bucureşti, 1980.
2. G i u r m a I., *Hidrologie şi hidrogeologie, aplicaţii*. Ed. "Gh. Asachi", Iaşi, 2001.
3. G i u r m a I., *Sisteme de gospodărirea apelo*r, Ed. Cermi, Iaşi, 2000.
4. M u s y A., *Hydrologie appliquée*, Ed. HGA, Bucureşti, 1998.
5. * * *, *Anuarele hidrologice pentru bazinul reprezentativ Ciurea din perioada 1991 – 2006,*
6. * * *, *Studii si cercetari hidrologice*, Ed. Inst. de Meteor. si Hidrol., *XLIX* (1980) Bucuresti

EVOLUŢIA PARAMETRILOR HIDROLOGICI ÎN BAZINUL REPREZENTATIV TINOASA-CIUREA, JUDEŢUL IAŞI

(Rezumat)

Se prezintă rezultatele observaţiilor şi măsurătorilor efectuate, pe o perioadă de 16 ani (1992-2007) în bazinul reprezentativ Tinoasa-Ciurea, judeţul Iaşi, asupra condiţiilor care concură la formarea debitelor lichide în reţeaua hidrografică.

BULETINUL INSTITUTULUI POLITEHNIC DIN IAŞI
Publicat de
Universitatea Tehnică „Gheorghe Asachi" din Iaşi
Tomul LIV (LVIII), Fasc. 2, 2008
Secţia
HIDROTEHNICĂ

MINIMIZATION OF ENERGETIC COSTS IN OPERATION OF WATER DISTRIBUTION SYSTEMS

BY

EMANOIL BÂRSAN and CĂLIN IGNAT

The energetic costs represent the most expenses for water supply systems working by pumping. The work presents a model for optimized control of water distribution systems operation. The proposed model establishes the working characteristics of a water distribution system (supplying flow rate and pumping head) in view of minimization of the pumping costs. Minimization of costs is realized by supplying flow rate and pumping head control.

Supplying flow rate control is realized by the minimization of maximum supplying flow rate in the 24 h of the day by rational utilization of tank storage capacity (which by it diameter and height significant influences this minimization). To this flow rate it may be introduced the supplementary conditions such as: the satisfaction of a minimum flow rate, a flow rate succession on hours which do not exceed as value a certain imposed size or the combination of these. Pumping head control is realized by the minimization of the reference piezometric head of piezometric surface so that the pressure at nodes to be comprised between minimum and maximum allowable values. The steps in flow rate and pumping head are: 1˚establishing of pumping flow rate by minimization of maximum supplying flow rate; 2˚ hydraulic calculation of network using supplying flow rate from the point 1˚; 3˚ establishing the pumping head by minimization of reference piezometric head.

The result model may be used to evaluate different schemes, tradeoffs between pumping and storage, improvement of operating efficiency and system reliability. The method may by used at any water distribution system which must optimize pumping operation and tank control and which proposes itself the integration of direct telemetric and optimal control systems with computer to reduce energetic costs and the realization of efficient operations

1. Introduction

Drinking and industrial water supply systems consume large quantities of electric energy that constitute, generally, the largest expenses for ost of these systems. Energetic costs are a function of consumed energy quantities and energy cost. Energetic costs are structured to promote the using of energy out of consuming peaks when the costs are less and penalization the energy using in peak periods when the costs are larger.

Measures for energy saving in water distribution systems may be realized in many kinds, beginning with field test and equipment maintenance up to using optimal control with computer. Energy utilization may be reduced by diminishing the water pumped volume (that is, adopting some limits for pressure zone), diminishing pumping head (that is the optimization of the series of water levels in tank) or energy price reducing (that is, the avoid of pumping in peak hours and using the storage tanks so that their filling to be out the peak period and their draining in time of peak period) and increasing of pumps efficiency (that is, assuring as the pumps operate near by best efficiency point). Water supply systems may reduce further the costs by implementation of the direct telemetry and control systems (Supervisory Control and Data Acquisition, SCADA) and energy consumption control using optimization of pumping and storing operations in tank.

In recent years there was done different attempts to develop the optimal control algorithms with the view to help the operating of complex water supply systems. With that end in view the linear, nonlinear and dynamic programming and enumeration techniques (genetic algorithms) are used. The grade and mode of application of these techniques depend on the complexity of system.

Recently for optimal exploitation of pumps from a water supply system was applied the enumeration techniques – genetic algorithms [3], that is, a program for hydraulic solving of a water supply system combined with a enumeration algorithm of problem solutions realized on the genetic base (reproduction, mutation).

This paper presents a proper modality to realize the pumping in water supply systems consisting of separate optimization of pumped flow and pumping head for minimization of pumping energetic costs in system during of 24 h.

2. Model formulation

Minimization of energetic costs in a distribution system made up from pumping station -distribution network – inflow/draining tank, is proposed to be realized with a model developed in three steps:

1. The network supply flow (and therefore pumping flow) is determined to assure optimal use of tank in the sense to bring from source a strict necessary water quantity to assure the flows at nodes on hours, in 24h. In this view it is added an auxiliary variable flowmax (**z**) for supplying flow rate in such way as flow t < flowmax in 24 h (t = 1,…,24). By minimization the flowmax is established hour by hour from the 24 h strict necessary supplying flow with optimal tank utilization.

More concrete: if done the network configuration (lengths and diameters on pipe and ground level at nodes) is known, consumptions in network at nodes in each hour from the 24 h of day and the tank by diameter D and height H, the minimization of the largest value of network hour supplying flow that assures the consumption at nodes is followed.

Consider the variable $\mathbf{x_1 .... x_{24}}$ the network supplying flows hour by hour during a day; $\mathbf{y_1 .... y_{24}}$ tank supplying or draining flows in the same time interval; $\mathbf{c_1 ..... c_{24}}$ network consumptions at nodes in 24 h and **z** a variable that means network supplying maximum flow (on hour).

In this step it is solved the following problem:

min **z**

with restrictions:

$\mathbf{x_t = c_t + y_t}$

$\mathbf{y_{t+1} - y_t} \leq$ tank volume/3,600

$\mathbf{z - x_t \geq 0}$ with t = 1,…..,24 h

In addition the supplying flow calculation may be done and setting the following conditions:

a – imposing of a minimum flow as a percent from the average consumption;

$\mathbf{x_t}$ > minimum flow (percent from average consumption);

b - imposing of a maximum difference between two successive hour supplying flows;

$\mathbf{x_{t+1} - x_t}$ < maximum difference imposed

c - combination of conditions (minim un of maxim un flow, minim un flow, maximum difference).

2. The network is balanced with the supplying flows established in the previons step (1) with methodology from [2]. It is determined the flows and head losses on pipes, the piezometric head at nodes, etc.

3. At the 3rd step, the reference head, $\mathbf{H_{ref}}$ needs for piezometric surface establishing is minimized. This must assure at nodes the pressure comprised between an imposed minimum and maximum (current nodes, i,adjacent ones, j):

$$\min \mathbf{H_{ref}}$$

$$\mathbf{H_i = H_j + h_{ij}}$$

$$\mathbf{H_i \geq ground\ level_i + p_{min}}$$

$$\mathbf{H_i \leq ground\ level_i + p_{max}}$$

with p_{min} and p_{max} – minimum and maximum imposed pressure in node i.

The calculation program establishes the minimum pumping flow and head for a given distribution system.

3. Application Example

Fig. 1 presents the distribution system considered for exemplification (pumping station (pipe 23 –1) – network (22 nodes) – inflow/draining tank (node 24)).

For the tank there exists a facility that permits the consideration of any type of tank There are taken in consideration the following types of cylindrical tanks (D - diameter; H - height) I - D = 27.5 m and H = 8 m ; II – D = 15 m , H = 6 m;

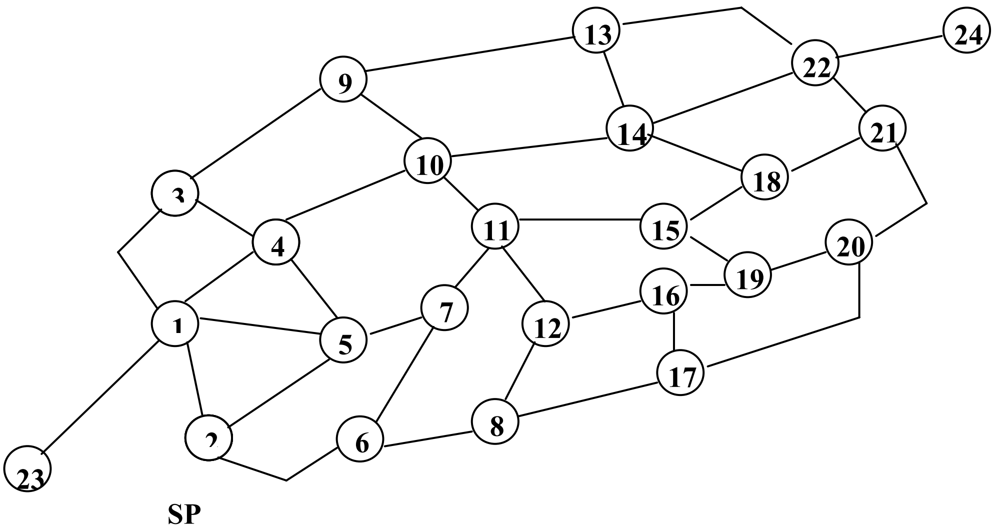

Fig. 1. Network graph.

In Fig. 2 is presented a screen for options that may be:

a) Tank position (by node), their dimensions (D and H).

b) Establishing of pumping flow and head by considering the minimization of maximum network hour supplying flow; taken into consideration a minimum flow (in percents from average flow); imposing of a maximum difference between two successive hour flow or combination of the anterior considerations.

For a tank disposed in node 24, with D = 15 m and H = 6 m and options from Fig. 2 (maximum flow, minimum flow, difference successive flows) the following graphs are presented:

Fig. 3. presents the supplying (by pumping) and consumption graph of network in 24 h. In Fig. 4 is presented, on hours, the pumping head;

Fig. 5 presents water level variation in tank but in fig. 6 it is presented the correlation between supplying flow and pumping head (necessary working point) of a pumping system (in 24 h) for choosing the type of pumps and running program.

Graphs from fig. 3, 4 and 6 serve for program establishing and pumping energy costs.

Authors have in view, for the near future, the realization of this stage with a computer program.

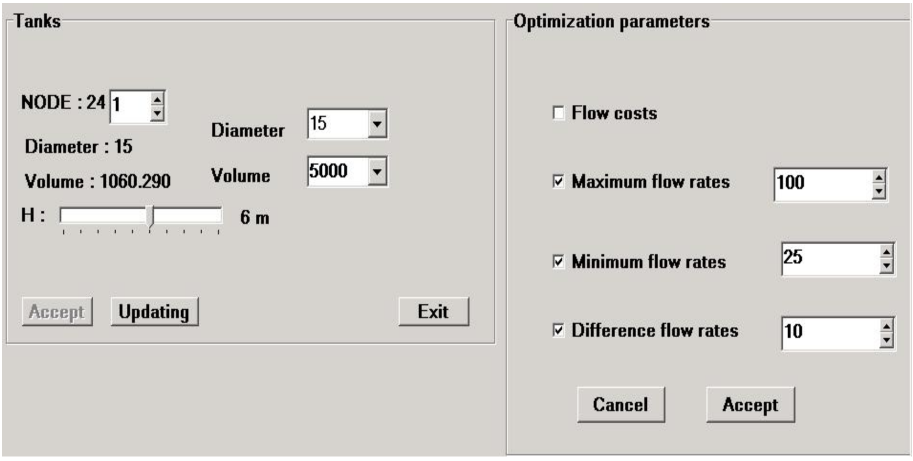

Fig 2. Optimization options

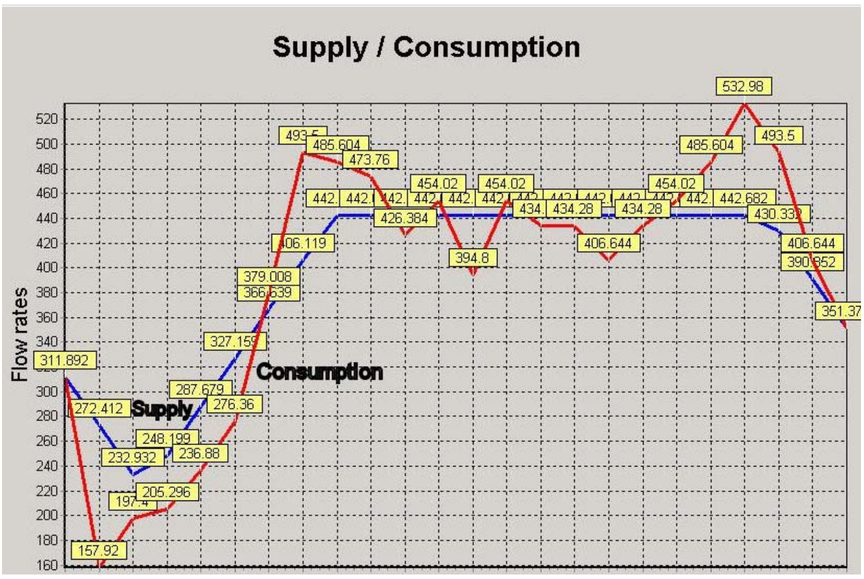

Fig. 3. Graph of network supply and consumption flow rates(L/s)

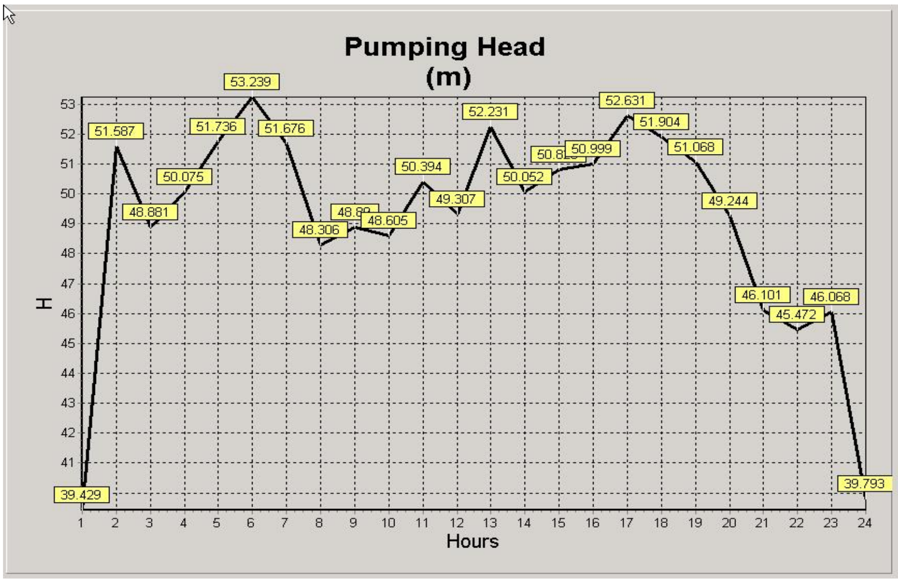

Fig. 4. Pumping head H (m) vs time, (h)

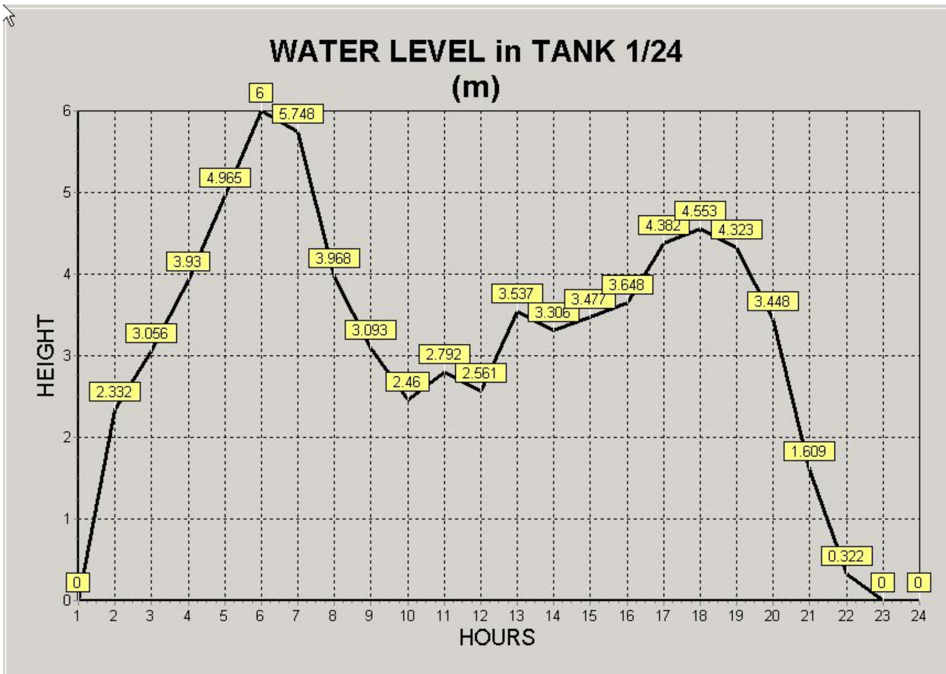

Fig.5.Water level in tank. head (height) vs. time, (h)

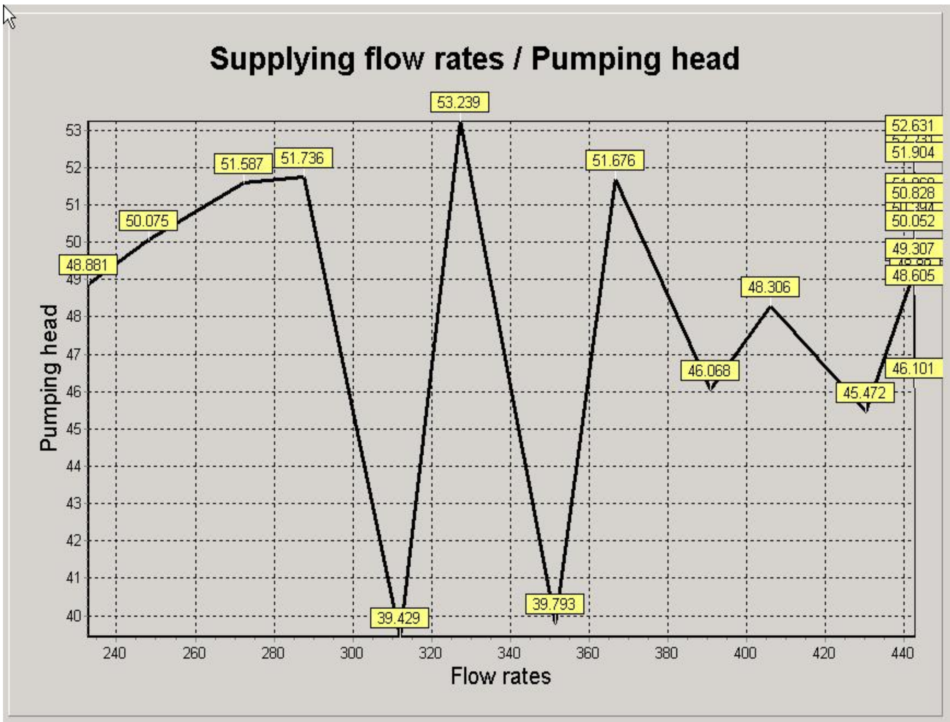

Fig. 6. Supplying flow rates vs. pumping head (H}. Oon abscissa – flow rates ; on ordinate – pumping head (H}

4.Conclusions

The work oposes model for establishing the pumping program and energetic costs in a supply system by pumping, developed in three stages:

1˚ establishing of pumping flow by minimization of maxim un supplying flow;

2˚ network hydraulic calculus using the supplying flow from point 1˚ ;

3˚ establishing of pumping head by minimization of referring piezometric head.

The proposed model contains the following facilities presented in Fig. 2.

a) options for tank position (by knot) and their dimensions (D and H);

b)options for minimization of maximum network hour supplying flow;

c)taken into consideration of minimum flow (in percents from average flow);

d) imposing of a maximum difference between two successive hour flows or combination of the anterior considerations.

The model was applied at the system presented in Fig. 1. In Fig. 3, 4, 5, 6, for a tank having D = 15 m and H = 6 m, are presented the supplying and consumption flows of network; the pumping head; the water level in tank and the correlation between supplying flow and pumping head of the considered system.

Received, June 4, 2008

"Gheorghe Asachi", Technical University, Jassy
Department of Hydrotechnical Structures and SanitaryEngineering
and"Al.I.Cuza", University , Jassy
Department of Applied Informatics

REFERENCES

1. Bârsan Em., Ignat C., *Technical-Economic Analysis of Water Distribution Networks*, Water Sci. & Technol.: Water Supply, London, 1, 2, 201-210, (2001)
2. Bârsan Em., Ignat C., *Sisteme de distributia apei*, Ed. Cermi Iaşi, 2001
3. Boulos P.F., Wu Z., Orr Ch.H., Moore M., Hsiung P., Thomas D., *Optimal Pump Operation of Water Distribution System Using Genetic Algorithm*, *RBF Consulting*, 2002
4. IWSA World Water Congress , 7 International Report, *State of the Art Regarding On-line Control and Optimization of Water Systems*, vol.1 I.R., Buenos Aires, 1999, IR-1- 45
5. Walski Th., Chase, D.V., Savic D.A., *Water Distribution Modeling*, Haestad Press, Waterbury, 2001.

.

MINIMIZAREA COSTURILOR ENERGETICE IN EXPLOATAREA SISTEMELOR DE DISTRIBUTIA APEI

(Rezumat)

Se prezintă o posibilitate a exploatării unui sistem de distribuția apei funcționând prin pompare în vederea micşorării costurilor energetice
Minimizarea costurilor se realizează prin controlul debitului de alimentare şi a înălțimii de pompare.

Controlul debitului de alimentare se realizează prin minimizarea debitului maxim de alimentare în cele 24 ore ale zile prin utilizarea rațională a capacității de înmagazinare a rezervorului (care prin diametrul şi înălțimea lui influențează semnificativ această minimizare). In plus, pentru stabilirea acestui debit se mai pot introduce condiții suplimentare cum ar fi: satisfacerea unui debit minim, o succesiune de debite pe ore care să nu depăşească ca valoare o anumită mărime impusă sau combinații ale acestora.

Controlul înălţimii de pompare se realizează prin minimizarea cotei piezometrice de referinţă a suprafeţei piezometrice aşa încât presiunile la noduri să fie cuprinse între valorile minime şi maxime admise.

Paşii în calculul debitului şi înălţimii de pompare sunt: 1˚stabilirea debitului de pompare prin minimizarea debitului maxim de alimentare; 2˚ calculul hidraulic al reţelei folosind debitul de alimentare de la punctul 1˚; 3˚ stabilirea înălţimii de pompare prin minimizarea cotei piezometrice de referinţă. Modelul care rezultă poate fi folosit pentru a evalua diferite scheme, a optimiza echilibrul pompare / înmagazinarea, îmbunătăţirea eficienţei de exploatare şi siguranţei sistemului. Metoda poate fi utilizată la orice sistem de alimentare cu apă funcţionând prin pompare care doreşte să optimizeze exploatarea pompării şi controlul rezervorului pentru a reduce costurile energetice ale exploatarii sistemului.

BULETINUL INSTITUTULUI POLITEHNIC DIN IAŞI
Publicat de
Universitatea Tehnică „Gheorghe Asachi” din Iaşi
Tomul LIV (LVIII), Fasc. 2, 2008
Secţia
HIDROTEHNICĂ

MONITORING THE EXPLOITATION OF THE INDUSTRIAL WASTE DUMP

BY

MIHAIL LUCA and RĂZVAN-PAUL BALAN

A method of monitoring the dumps of wastes resulting from the iron and steel industry and their impact on the environment. The case study carried out at a metallurgical group of enterprises emphasizes the negative impact of the waste dumps on the environment. The monitoring was performed on the following fields: the wastes storage in the environment, the operation of the dump, the impact on the environment etc. The analysis carried out referred to the dumps running and the ones in conservation. The new regulations regarding the environmental agents monitoring and the ecologic reconstruction of the area, an studiu too.

1. Introduction

The environment represents the totality of the *Earth* natural components as well as their living conditions. The components are defined by air, water, soil and subsoil, flora, fauna, by the social human values established in time and the interactions between such components etc. Pollution is a process by which the biotic and non-biotic environments are altered but which affects also the values created by the human society, being caused by human activities. Furthermore, contamination may also involve an environmental degradation caused by natural agents.

One of the 13 domains regulated by the environmental IQ is represented by the vast and complex domain of “waste management” which comprises specific regulations regarding industrial waste dumps.

Industrial waste dumps must be endowed with control and measurement equipment in order to measure the parameters considered in the analysis. The behavior in time of the running dump should be monitored following to the new regulations adopted in the field. Due to the high construction, operation and monitoring costs of a controlled waste dump both during its filling and during its conservation, a cost-profit analysis is expedient. This analysis will represent a criterion in selecting the storage area and the construction solution of the dump. According to the provisions in force in the European Union the storage prices should cover the closure, operation and monitoring costs for a period of minimum 50 years after the dumps closure.

2. Technological Processes in the Industrial Waste Dumps

The case study was performed on the industrial waste dumps belonging to Mittal Steal Group Galati.

Important quantities of waste more or less toxic depending on their nature which cause big problems as regards their processing and storage result from the industrial processes carried out within the Metallurgical Group of Enterprises Galați (S.C. ARCELOR MITTAL S.A. Galați). Their valorization was performed periodically, the useful substances being recovered and used for other purposes. In many cases these wastes were deposited in inadequate conditions, without previously preparing the ground; the wind and rains often transported these wastes to large areas and infested the underground waters and the surface waters, the environment being thus seriously damaged.

The slag dump analysed is located in the Western side of the metallurgical group of enterprises and neighbors Malina Bog to the North and the exploitation road of Şendreni Mayoralty to the East. The location of the dump starts at an altitude of 10.00 m on a table land situated between Cătuşa and Mălina Valleys and the farm lands of the localities Smârdan and Movileni.

The dump occupies a surface of approx. 110 ha. The average height of the dump is of approx. 50 m. The height varies surface-wise depending on the dump exploitation degree. In some sectors of the dump holes were formed due to the slag exploitation. The surrounding land, situated outside the perimeter approved for storage is partially and even totally covered with wastes.

The dump which is situated in the Western part of the unit first occupied the Eastern side of Mălina Lake and advanced towards other directions covered with water. The advance was horizontal, but also with a continuous slope and if in the beginning the elevation marks were 40…46 m height they reached 60 m in the unloading faces area.

The construction of the slag dump started in 1968. The wastes resulting from the technological process of the Metallurgical Group of Enterprises Galați (Fig.1) were stored there.

Fig. 1. The industrial waste dump in operation phase

The execution project based on which the waste dump was built is no longer available.

The analysis carried out within the dump for 5 years pointed out the following risk situations:

a) there is no natural or artificial waterproofing;

b) the waste dump has no drainage system for the leachate collection and treatment;

c) there are no collecting channels for meteoric water;

d) the waste dump has no gas collection and disposal system;

e) the dump slopes are instable;

f)meteoric waters infiltrated into the dump are not collected and drained through an appropriate drainage system;

g) the subsurface waters are polluted by uncontrolled infiltrations from the waste dump;

h) the access in the dump is free, etc.

The metallurgical group's operation is in direct relation with the evacuation and storage of the wastes. Due to the quality parameters but also from technical-economical reasons the wastes cannot be revaluated.

The wastes have been stored there for a lot of time and this is why a relief currently called "slag dump" appeared next to the unit.

36,50 mil tones of blast furnace slag and approx. 14, 50 mil.t of steel plant slag were deposited on the slag dump location during the 1968…2006.

They were stored on the surface of the period dump on a more or less selective basis. Initially the surface of the deposit was smaller but by successive deposits the actual surface exceeded the designed one. Despite this, there have not been taken neither waterproofing measures for the extended base of the dump nor measures meant to ensure the leachate draining and disposal system.

3 mil t of blast furnace slag, 1.50 mil t of steel plant slag and 600.000 t of other wastes have been deposited in the dump during the 2003…2006 period. An estimated share of the stockpiled materials is the following:

a) blast furnace slag – approx. 47%;
b) steel plant slag – approx. 30%;
c) refractory wastes and other – approx. 23%.

The volumetric density of stockpiled material is of an average of approx. 2,100 kg/m^3.

The industrial wastes dump and the technological processes carried out on site do not generate residual waters. The used water resulting from the slag granulation is collected by the sewage system of the metallurgical group.

The meteoric waters infiltrating into the material stored infiltrate into the soil where from they get into the ground water and then into the emissary (Mălina Bog). At the same time the waters draining on the dump slope determine its erosion, whereupon they draw off into Mălina Bog. Part of this water is absorbed by the mass of the dump or by the soil in the adjacent area. The infiltrated water influences the quality of the subsurface water and of the water in Mălina Bog.

Mălina Sud sludge bed situated in the Southern part of the dump helps the used waters from the blast furnace and steel plant slag taken over by C8 collector discharge in Mălina Bog.

Since there is no draining and collecting system of the leachate generated by the percolation of the dump by the meteoric waters, the slag dump through its position influences both the quality of the subsurface water and the emissary (Mălina Bog).

Because the storage and distribution surface of the industrial wastes has exceeded the Western bounds of the dump, the escarpment of the dump registered some landslips between 2004 and 2005. This phenomenon generated silting processes and even the obstructing of the sewer in Mălina Nord area.

3.The Storage Technology

In order to deposit the wastes in the slag bank the automotive transport is used for the blast furnace and steel plant slag. In order to deposit the refractory and industrial wastes, the railway transport is used. The blast furnace non-granulated slag, cooled and solidified is transported and deposited in the slag dump on platforms, a new stage being thus created, the access being possible on the previously deposited wastes.

The truck unloading face is situated in the N-W side, on the marginal line of the slope. The bank slope is consolidated only by the compaction exercised by the trucks weight. The waste trucks are side-tracked, blocked and then dumped. When the slope has achieved its back angle and the wastes no longer slip towards the base, a dozer compaction is performed and the infrastructure towards the area of the new slope is prepared (Fig. 2).

The infrastructure of the new unloading railway face is made of various types of wastes with different granulations. This procedure is adopted because the effect of the slope upon loading is unknown and slide surfaces may appear. It is worth mentioning that in the access area where the wastes transport is done by railway, the storage was not selective. Various types of materials and wastes are met in this area.

At present the wastes storage is done on a surface of 84 ha, with the recommendation that the existing limit of the dump should be observed (Fig. 3).

The waste storage dumps are hydrotechnical constructive structures which involve some special technical-economical and social aspects, such as.

a) ensuring the stability and preventing the possible accidents which may take place by the industrial wastes displacement as well as by their forming structure breaking;

b) collecting the surface and subsurface waters with their treatment where necessary;

c) preventing the contamination of the environment with substances carried off from the dumps;

d) the reintegration of the land used for deposits into the economic and ecologic circuit.

Fig. 2. Unloading face for the industrial wastes.

Fig. 3. The compaction and leveling of the industrial wastes storage face.

The legislation in force on which governs the design, the operation and closure (abandon or conservation) of the dumps (waste bank) is very vast, the most important being.

a) GUO 244/2000 amended and completed with the Law 466/2001 regarding the safety of the dams;

b) 426/2001 – Law for the approval of the Government Urgent Ordinance no. 78/2000, regarding waste regime;

c) the Order of the Minister of Waters and Environment Protection no. 1147/2002 for the approval of the Technical Standard Regarding Wastes Storage – the construction, running, monitoring and closure of the waste dumps;

d) 867/2002 - the Order of the Minister of Waters and Environment Protection regarding the definition of the criteria that wastes must fulfill in order to appear on the national list of accepted wastes from each class of waste dumps;

e) 162/2002 – the Decision of the Government no regarding the wastes storage.

The environment legislation in force regarding the construction, monitoring and closure of the waste dumps, includes specific recommendations regarding the necessary data and information for each stage of the dump life cycle.

4. The Slag Dump Running and the Environment Agents Monitoring

The technological monitoring is carried out during the entire operation duration of the dump and is essential for its good running. Thus the risk of accidents and destruction of the waterproofing bed is reduced. The working order of all the dump components should be permanently controlled: the access road and the one in the precincts, the condition of the existent endowments, the degree of settlement and the stability of the dump, the control of the waste entrances (consignment notes, making the conformity analyses), etc. (Fig 4).

Fig. 4. – Recovering the industrial wastes.

For a strict surveillance of the wastes bank running the strict monitoring of the liquid, gas and solid emissions is necessary. Its object is to check if the emissions comply with the competent authorities' requirements (the environment and the water utilization authorization).

The monitoring process of the subsurface waters is carried out for the following parameters: pH, suspensions, fixed residue, CCOCr, chlorides, sulphates, nitrates, ammonium, Fe, Ca, Mg, phenols, cyanides, Cr, Zn, Mn, Pb, Ni. Each month samples are taken from the observation drillings executed on the site and in the neighborhood. The samples are analys and the results are compared with the values imposed by the standards and norms in force.

In order to monitor the underground water, two drillings executed down at a depth of 21 m are used.

The quality of the environmental agents from the influence area of the wastes dump is controlled having in view.

a) the registration of the meteorological data obtained from the local weather station on a monthly basis in order to establish the quantity of precipitations, the temperature and the prevailing direction of the wind;

b) determining the concentrations of the specific markers in the environmental air from the dump influence area (sedimentation powders – monthly, aerosols – monthly samples);

c) determining the noise level during the operations which require blasting and during the wastes unloading and ecologization works (tow quarterly determinations);

d) determining the specific concentration of pollutants in the soil from the dump influence area (pH, SO4, Cd, Mn, Pb four samples taken from the four cardinal points per semester).

Due to the nature of the wastes and the storage technology used, the material which makes the structure of the slag dump is very inhomogeneous both physically and chemically. On the other hand, the dump has impressive dimensions both in horizontal and vertical plane. Therefore, a characterization of its physical chemical composition by lab analyses would take a lot of time and the conclusions would be irrelevant and uncertain. Consequently, it seemed expedient to take samples from the material stored, the wastes being characterized by the analyses performed by the producer.

The soil samples were taken from the neighboring area next to the bank from four points (two samples for every one: a surface one and one 30 cm deep) situated approximately on the four cardinal directions in respect to the dump. The dump position as well as the predominant wind direction in the area was considered. The choice of the four sampling points allows the analysis of the polluting effect of the dump activity on the soil.

Considering the nature and the chemical composition of the wastes deposited and the recommendations in annex 3.1 to the MAPPM Order 184/1997, the lab analysis of the soil samples aimed to determine the heavy metals (Pb, Cd and Mn), sulphates and pH concentration.

In order to appreciate the wastes dump contamination effect, the results of the analyses performed on the soil samples taken from the East side of the location in June July 2006 are presented in Table 1.

Table 1

Contamination Effect of the Wastes Dump

Soil sample code	Determined parameters				
	pH	Cd mg/kg	Mn mg/kg	Pb mg/kg	SO_4^{2-} mg/kg
Less sensitive possessions (inside the metallurgical unit)					
E/ surface	8.18	1.42	1.370	53.2	460.2
E / 30 cm	8.20	1.58	1.399	46.7	880.2
Normal values (Ord. 756/1997)	-	1	900	20	-
Alert threshold (Ord. 756/1997)	-	5	2.000	250	5.000
Intervention threshold (Ord. 756/1997)	-	10	4.000	1000	50.000

Less sensitive possessions (outside the metallurgical unit)					
E/ surface	8,26	1.61	1.270	38.2	601.4
E / 30 cm	8,22	1.83	1.184	37.5	909.8
Normal values (Ord. 756/1997)	-	1	900	20	-
Alert threshold (Ord. 756/1997)	-	3	1.500	50	2.000
Intervention threshold (Ord. 756/1997)	-	5	2.500	100	10.000

From the analysis of the data it results that the soil samples have a pH value of over 8,50, what confers to the soil in the area an alkaline character. The concentration of the lead in all the analys samples exceeds the normal values without exceeding however the intervention threshold for the sensitive utilities.

Considering the position of the sampling points with respect to the slag dump and the predominant direction of the wind the negative effect of its activity on the soil is obvious.

Presently S.C. MITTAL STEEL S.A. manages selectively the slag wastes. Distinct areas for wastes storage were arranged. In the following period the utmost utilization of the wastes will be achieved by the excavation and processing of the slag in the dump, without affecting however the stability and safety of the dump. The wastes which cannot be valuated shall be stored in distinct area in a controlled and selective manner, according to the technology.

During 2005-2006 the granulation of the blast furnace slag was done up to more than 70% of the slag quantity produced so that no slag would be stored in the dump.

5. The Post Closure Monitoring and the Ecologic Reconstruction of the Area Affected by the Industrial Waste Storage

In order to comply with the environment protection requirements regarding the closure of the slag dump, the following measures should be taken:

a) the final coverage of the dump under safety conditions considering the previous land utility and the landscape framing;

b) monitoring the emissions into the environment after the actual closure of the dump for minimum four years until the complete stabilization of the wastes.

The layers of the covering system must ensure.

a) the stabilization of the wastes;
b) the subsequent use of the land;
c) waterproofing layer;
d) layer for collecting and disposing the rain waters;
e) vegetal soil layer.

According to the legal provisions, the dump operator is obliged to ensure the post-closure monitoring for the period established by the competent environment authority (min. three years). The post-closure monitoring system shall be performed for 4 years and shall comprise the meteorological data, the concentrations of pollutants in the soil, underground water and air, together with a careful monitoring of the subsurface water quality parameters. At the same time, topographical studies on the stability of the slag dump shall be performed by using the landmarks mounted on the dump platform and on the slope.

After turning to good account part of the slag dump, ecologization technologies shall be applied for the volume remained unvalued after extracting the iron. The works include putting back the slag dump into the forest circuit and shall be done by stages.

The ecological reconstruction of the wastes dump shall be considered completed based on some evaluation criteria regarding.

a) the quality of the environment agents;

b) the wastes settling;

c) possibilities of subsequently using the ecologically rebuilt land.

The subsequent use of the location shall be done considering the specific conditions and restrictions imposed by the existence of the covered dump depending on the stability of the land and the degree of risk it may present for the environment and human health.

6. Conclusions

1. In order to make the industrial waste dumps safe the regulations in the field correlated with the European law provisions shall be observed.

2. The slag dumps resulting from the metallurgical and syderurgical groups require special attention due to the components included. They influence significantly the stability and circulation of the surface and subsurface waters.

3. The dump safing must be carried out during the operation stage by adopting measures meant to allow a controlled expansion and super-elevation of the dump but without affecting and polluting the environment of the location. The research carried out in this case study indicates various contamination stages of the surface and subsurface waters.

4. During the operation and conservation stage the permanent monitoring of the parameters specific to the dump as well as of the location environment should be performed in order to reduce to a minimum the environmental contamination.

5. Both during the dump operation and conservation stage the location area should undergo an ecologization.

Received, June 4, 2008

"Gheorghe Asachi" Technical University Jasy,
Department of Hydrotechnical Constructions and Sanitary Engineering Department
" National Administration,of Romanian Waters Prut Directorate Jasy

R E F E R E N C E S

1. C h a r b e n e a u R.J., *Groundwater Hydraulics and Pollution Transport*. Prentice Hall, New Jersey, SUA, 2000;
2. D a v i d I., Ş u m ă l a n I., C a r a b e t A., N i ţ u ş c ă A., *The Transport of the Pollutants through Fluid Mediums,* Edit. Tehnică, Timişoara, 1998;
3. L u c a M., *Considerations Regarding the Pollution Phenomenon Induced by the Dirt Heaps*, Intern. Conf. „Disaster and Pollution Monitoring" "Gh. Asachi" Technical Univ. Jasy, 2004;
4. M a r c h i d a n u E., *Hydrogeology in Construction Engineering*, Edit. Tehnică , Bucureşti, 1996;
5. M ă n e s c u S., M a n o l e C., D i a c o n e s c u M. L., *Environment Sanitary Chemistry (1978),* Edit. Tehnică , Bucureşti;
6. S t e m a t i u D., – *Mud-Setting Ponts – Risk Management*, Edit. House MATRIX ROM, Bucureşti, 2002;
7. A p p e l o C.A.J., P o s t m a D. *(1996) Geochemistry,Grounwater and Pollution*. Balkema Edit. Tehnică ;
8. D r e v e r J. I. *The Geochemistry of Natural Waters. Surface and Groundwater Environments,* Prentice Hall, NZ,1997;
9. P â r v u C., *General Ecology (2001),* Edit. Tehnică , Bucureşti,2001;
10. * * * *Technical Documents, Studies and Analyses* - S.C. ARCELOR MITTAL S.A. Galaţi.

MONITORIZAREA EXPLOATĂRII DEPOZITELOR DE DEŞEURI INDUSTRIALE

(Rezumat)

Lucrarea prezintă modul de monitorizare a depozitelor de deşeuri rezultate din industria siderurgică şi impactul acestora asupra mediului. Studiul de caz efectuat la un combinat metalurgic pune în evidenţă impactul negativ a depozitelor de deşeuri asupra mediului. Monitorizarea s-a realizat pe domeniile: stocarea deşeurilor în mediu, exploatarea depozitului, impactul asupra mediului etc. Analiza efectuată s-a referit la depozitele aflate în exploatare şi a celor aflate în conservare. Lucrarea analizează şi reglementările noi privind monitorizarea factorilor de mediu şi la reconstrucţia ecologică a zonei.

BULETINUL INSTITUTULUI POLITEHNIC DIN IAŞI
Publicat de
Universitatea Tehnică „Gheorghe Asachi" din Iaşi
Tomul LIV (LVIII), Fasc. 2, 2008
Secţia
HIDROTEHNICĂ

ANALYSIS OF THE CLIMATIC CHANGES PERSPECTIVES USING MATHEMATICAL MODELS

BY
Catrinel-Raluca GIURMA-HANDLEY, I.CRACIUN and M.TELISCA

The purpose of this paper is to assess and quantify projections of possible future climate change from climate models. There are analyzed various possibilities and also the possible responses under the pressure of the environmental factors that affect the climate variations.

1. Introduction

A background of concepts used to assess climate change experiments is presented in the paper which includes results from ensembles of several categories of future climate change experiments, factors that contribute to the response of those models, changes in variability and changes in extremes. In a departure from the organization of the Second Assessment Report (IPCC, 1996) (hereafter SAR), the assessment of regional information derived in some way from global models (including results from embedded regional high resolution models, downscaling, etc.).

2. Background and Recap of Previous Reports

Studies of projections of future climate change use a hierarchy of coupled ocean/atmosphere/sea-ice/land-surface models to provide indicators of global response as well as possible regional patterns of climate change. One type of configuration in this climate model hierarchy is an Atmospheric General Circulation Model (AGCM), with equations describing the time evolution of temperature, winds, precipitation, water vapors and pressure, coupled to a simple non-dynamic "slab" upper ocean, a layer of water usually around 50 m thick that calculates only temperature (sometimes referred to as a "mixed-layer model"). Such air-sea coupling allows those models to include a seasonal cycle of solar radiation. The sea surface temperatures (SSTs) respond to increases in carbon dioxide (CO_2), but there is no ocean dynamical response to the changing climate. Since the full depth of the ocean is not included, computing requirements are relatively modest so these models can be run to equilibrium with a doubling of atmospheric CO_2. This model design was prevalent through the 1980s, and results from such equilibrium simulations were an early basis of societal concern about the consequences of increasing CO_2.

However, such equilibrium (steady-state) experiments provide no information on time-dependent climate change and no information on rates of climate change. In the late 1980s, more comprehensive fully coupled global ocean/atmosphere/sea – ice/land – surface climate models (also referred to as Atmosphere-Ocean Global Climate Models, Atmosphere-Ocean General Circulation Models or simply AOGCMs) began to be run with slowly increasing CO_2 , and preliminary results from two such models appeared in the 1990 IPCC Assessment (IPCC, 1990).

In the 1992 IPCC update prior to the Earth Summit in Rio de Janeiro (IPCC, 1992), there were results from four AOGCMs run with CO_2 increasing at 1%/yr to doubling around year 70 of the simulations (these were standardized sensitivity experiments, and consequently no actual dates were attached). Inclusion of the full ocean meant that warming at high latitudes was not as uniform as from the non-dynamic mixed-layer models. In regions of deep ocean mixing in the North Atlantic and Southern Oceans, warming was less than at other high latitude locations. Three of those four models used some form of flux adjustment whereby the fluxes of heat, fresh water and momentum were either singly or in some combination adjusted at the air-sea interface to account for incompatibilities in the component models. However, the assessment of those models suggested that the main results concerning the patterns and magnitudes of the climate changes in the model without flux adjustment were essentially the same as in the flux-adjusted models.

3. The Second Assessment Report of IPCC

The most recent IPCC Second Assessment Report (IPCC, 1996) included a much more extensive collection of global coupled climate model results from models run with what became a standard 1%/yr CO_2 -increase experiment.

These models corroborated the results in the earlier assessment regarding the time evolution of warming and the reduced warming in regions of deep ocean mixing. There were additional studies of changes in variability in the models in addition to changes in the mean, and there were more results concerning possible changes in climate extremes. Information on possible future changes of regional climate was included as well.

The SAR also included results from the first two global coupled models run with a combination of increasing CO_2 and sulphate aerosols for the 20th and 21st centuries. Thus, for the first time, models were run with a more realistic forcing history for the 20th century and allowed the direct comparison of the model's response to the observations. The combination of the warming effects on a global scale from increasing CO_2 and the regional cooling from the direct effect of sulphate aerosols produced a better agreement with observations of the time evolution of the globally averaged warming and the patterns of 20th century climate change. Subsequent experiments have attempted to quantify and include additional forcing for 20th century climate**,** with projected outcomes for those forcing in scenario integrations into the 21st century discussed below.

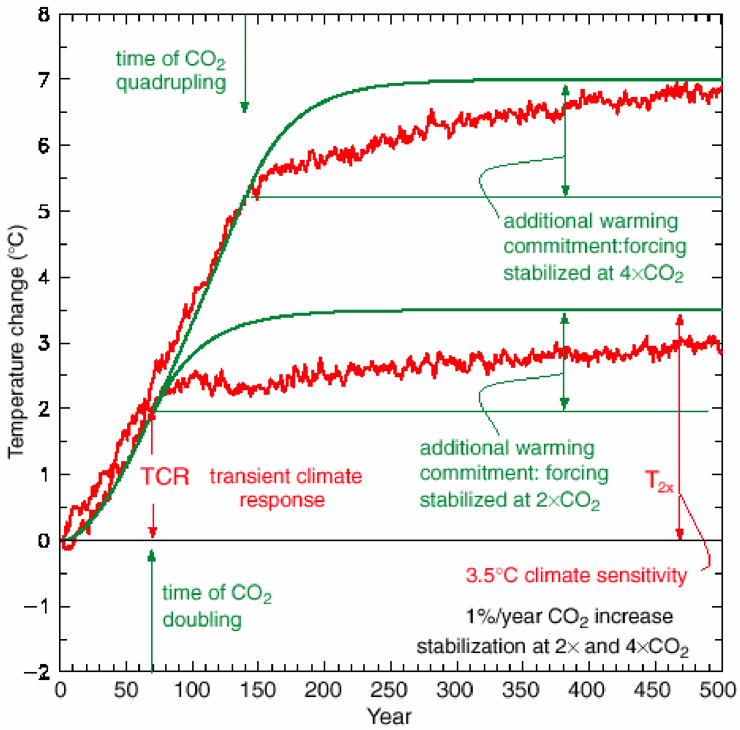

Fig. 1 Global mean temperature change for 1%/yr CO_2 increase with subsequent stabilization at $2CO_2$ and $4CO_2$. The red curves are from a coupled AOGCM simulation (GFDL_R15_a) while the green curves are from a simple illustrative model with no exchange of energy with the deep ocean. The "transient climate response", TCR, is the temperature change at the time of CO_2 doubling and the "equilibrium climate sensitivity", T2x , is the temperature change after the system has reached a new equilibrium for doubled CO_2 , i.e., after the "additional warming commitment" has been realized.

In the SAR, the two global coupled model runs with the combination of CO_2 and direct effect of sulphate aerosols both gave a warming at mid-21st century relative to 1990 of around 1.5°C. To investigate more fully the range of forcing scenarios and uncertainty in climate sensitivity (defined as equilibrium globally averaged surface air temperature increase due to a doubling of CO_2,) a simpler climate model was used. Combining low emissions with low sensitivity and high emissions with high sensitivity gave an extreme range of 1 to 4.5°C for the warming in the simple model at the year 2100 (assuming aerosol concentrations constant at 1990-levels). These projections were generally lower than corresponding projections in IPCC (1990) because of the inclusion of aerosols in the pre-1990 radiative forcing history. When the possible effects of future changes anthropogenic aerosol as prescribed in the IS92 scenarios were incorporated this led to lower projections of temperature change of between 1°C and 3.5°C with the simple model. Spatial patterns of climate change simulated by the global coupled models in the SAR corroborated the IPCC (1990) results. With increasing greenhouse gases the land was projected to warm generally more than the oceans, with a maximum annual mean warming in high latitudes associated with reduced snow cover and increased runoff in winter, with greatest warming at high Northern latitudes. Including the effects of aerosols led to a somewhat reduced warming in middle latitudes of the Northern Hemisphere and the maximum warming in northern high latitudes was less extensive since most sulphate aerosols are produced in the Northern Hemisphere. All models produced an increase in global mean precipitation but at that time there was little agreement among models on changes in storminess in a warmer world and conclusions regarding extreme storm events were even more uncertain.

4. New Types of Model Experiments

The progression of experiments including additional forcing has continued and new experiments with additional greenhouse gases (such as ozone, CFCs, etc., as well as CO_2) will be assessed in this paper.

In contrast to the two global coupled climate models in the 1990 Assessment, the Coupled Model Intercomparison Project (CMIP) [1] includes output from about twenty AOGCM's worldwide, with roughly half of them using flux adjustment. Nineteen of them have been used to perform idealised 1%/yr CO_2 -increase climate change experiments suitable for direct intercomparison and these are analyzed here. Roughly half that number has also been used in more detailed scenario experiments with time evolutions of forcing including at least CO_2 and sulphate aerosols for 20th and 21st century climate. Since there are some differences in the climate changes simulated by various models even if the same forcing scenario is used, the models are compared to assess the uncertainties in the responses. The comparison of 20th century climate simulations with observations has given us more confidence in the abilities of the models to simulate possible future climate changes in the 21st century and reduced the uncertainty in the model projections.

The newer model integrations without flux adjustment give us indications of how far we have come in removing biases in the model components. The results from CMIP confirm what was noted in the SAR in that the basic patterns of climate system response to external forcing are relatively robust in models with and without flux adjustment [2]. This also gives us more confidence in the results from the models still using flux adjustment. The IPCC data distribution centre (DDC) has collected results from a number of transient scenario experiments. They start at an early time of industrialization and most have been run with and without the inclusion of the direct effect of sulphate aerosols. Note that most models do not use other forcing such as soot, the indirect effect of sulphate aerosols, or land-use changes. Forcing estimates for the direct effect of sulphate aerosols and other trace gases included in the DDC models. Several models also include effects of tropospheric and stratospheric ozone changes. Additionally, multi-member ensemble integrations have been run with single models with the same forcing. So-called "stabilization" experiments have also been run with the atmospheric greenhouse gas concentrations increasing by 1%/yr or following an IPCC scenario, until CO_2 -doubling, tripling or quadrupling.

The greenhouse gas concentration is then kept fixed and the model integrations continue for several hundred years in order to study the commitment to climate change. The 1%/yr rate of increase for future climate, although larger than actual CO_2 increase observed to date, is meant to account for the radiative effects of CO_2 and other trace gases in the future and is often referred to as "equivalent CO_2". This rate of increase in radiative forcing is often used in model intercomparison studies to assess general features of model response to such forcing.

The IPCC began the development of a new set of emissions scenarios, effectively to update and replace the well-known IS92 scenarios. The approved new set of scenarios is described in the IPCC Special Report on Emission Scenarios (SRES) [3]. Four different narrative storylines were developed to describe consistently the relationships between emission driving forces and their evolution and to add context for the scenario quantification. The resulting set of forty scenarios (thirty-five of which contain data on the full range of gases required for climate modeling) cover a wide range of the main demographic, economic and technological driving forces of future greenhouse gas and sulphur emissions. Each scenario represents a specific quantification of one of the four storylines. All the scenarios based on the same storyline constitute a scenario "family". The SRES scenarios do not include additional climate initiatives, which means that no scenarios are included that explicitly assume implementation of the UNFCCC or the emissions targets of the Kyoto Protocol.

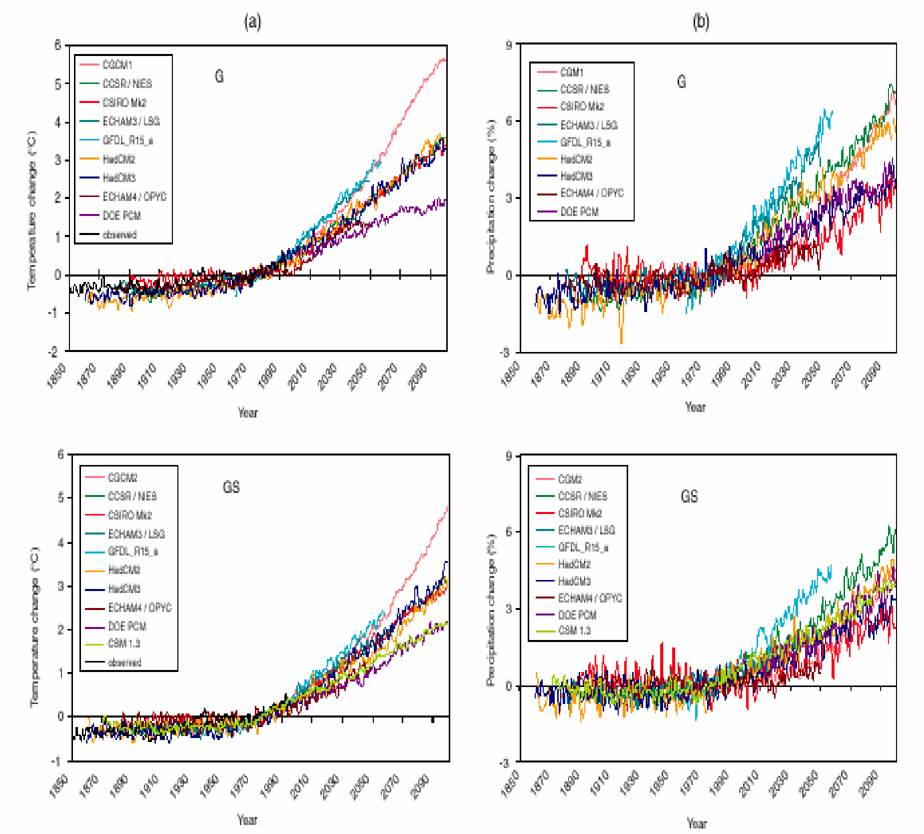

Fig. 2 (a) The time evolution of the globally averaged temperature change relative to the years (1961 to 1990) of the DDC simulations (IS92a). G: greenhouse gas only (top), GS: greenhouse gas and sulphate aerosols (bottom). The observed temperature change (Jones, 1994) is indicated by the black line. (Unit: °C). (b) The time evolution of the globally averaged precipitation change relative to the years (1961 to 1990) of the DDC simulations. GHG: greenhouse gas only (top), GS: greenhouse gas and sulphate aerosols (bottom). (Unit: %). See Table 9.1 for more information on the individual models used here.

Furthermore, government policies can, to varying degrees, influence the greenhouse gas emission drivers and this influence is broadly reflected in the storylines and resulting scenarios. Because SRES was not approved until 15 March 2000, it was too late for the modeling community to incorporate the scenarios into their models and have the results available in time for this Third Assessment Report. Therefore, in accordance with a decision of the IPCC Bureau in 1998 to release draft scenarios to climate modelers (for their input to the Third Assessment Report) one marker scenario was chosen from each of four of the scenario groups based on the storylines. The choice of the markers was based on which initial quantification best reflected the storyline, and features of specific models. Marker scenarios are no more or less likely than any other scenarios but these scenarios have received the closest scrutiny. Scenarios were also selected later to illustrate the other two scenario groups. These latter two illustrative scenarios were not selected in time for AOGCM models to utilize them in this report. In fact, time and computer resource limitations dictated that most modeling groups could run only A2 and B2, and results from those integrations are evaluated. However, results for all six illustrative scenarios are shown here using a simple climate model discussed below. The IS92a scenario is also used in a number of the results presented in order to provide direct comparison with the results in the SAR.

The final four marker scenarios contained in SRES differ in minor ways from the draft scenarios used for the AOGCM experiments described in this report. In order to ascertain the likely effect of differences in the draft and final SRES scenarios each of the four draft and final marker scenarios were studied using a simple climate model tuned to the AOGCMs used in this report. For three of the four marker scenarios (A1B, A2 and B2) temperature change from the draft and final scenarios are very similar. The primary difference is a change of the standardized values for 1990 to 2000, which is common to all these scenarios.

This results in a higher forcing early in the period. There are further small differences in net forcing, but these decrease until, by 2100, differences in temperature change in the two versions of these scenarios are in the range 1% to 2%. For the B1 scenario, however, temperature change is significantly lower in the final version, leading to a difference in the temperature change in 2100 of almost 20%, as a result of generally lower emissions across the full range of greenhouse gases.

5. Precipitation and convection

Increased intensity of precipitation events in a future climate with increased greenhouse gases was one of the earliest model results regarding precipitation extremes, and remains a consistent result in a number of regions with improved, more detailed models [4]. There have been questions regarding the relatively coarse spatial scale resolution in climate models being able to represent essentially mesoscale and smaller precipitation processes. However, the increase in the ability of the atmosphere to hold more moisture, as well as associated increased radiative cooling of the upper troposphere that contributes to destabilization of the atmosphere in some models, is physically consistent with increases in precipitation and, potentially, with increases in precipitation rate.

As with other changes, it is recognized that changes in precipitation intensity have a geographical dependence. For example the range of precipitation intensity over the South Asian monsoon region broadens in a future climate experiment with increased greenhouse gases, with decreases prevalent in the west and increases more widespread in the East [5]. Another model experiment [6] shows that extreme values of the convective rain rate and the maximum convective height occur more frequently during the 2071 to 2080 period than during the 1981 to 1990 period. The frequency of highest-reaching convective events increases, and the same holds for events with low cloud-top heights. In contrast, the frequency of events with moderate-top heights decreases. On days when it rains, the frequency of the daily rates of convective rainfall larger than 40 mm/day in JJA and greater than 50 mm/day for DJF, increases. Generally, one finds a strong increase in the rain rate per convective event over most of the land areas on the summer hemispheres and in the inter-tropical convergence zone (ITCZ).

Between 10° and 30°S there are decreases in rain rate per event over the ocean and parts of the continents. In global simulations for future climate, the percentage increase in extreme (high) rainfall is greater than the percentage increase in mean rainfall [7]. The return period of extreme precipitation events is shortened almost everywhere [8]. For example, they show that over North America the 20-year return periods are reduced by a factor of 2 indicating that extreme precipitation of that order occurs twice as often.

Another long- standing model result related to drought (a reduction in soil moisture and general drying of the mid-continental areas during summer with increasing CO_2) has been reproduced with the latest generation of global coupled climate models [9]. This summer drying is generally ascribed to a combination of increased temperature and potential evaporation not being balanced by precipitation. To address this problem more quantitatively, a global climate model with increased CO_2 was analyzed to show large increases in frequency of low summer precipitation, the probability of dry soil, and the occurrence of long dry spells [10].

The latter was ascribed to the reduction of rainfall events in the model rather than to decreases in mean precipitation. However, the magnitude of this summer drying response may be related to the model's simulation of net solar radiation at the surface, and more accurate simulation of surface fluxes over land will increase confidence in the GCM climate changes.

6. Conclusions

The following findings from the models analyzed in this chapter corroborate results from the SAR (projections of regional climate change are given in Chapter 10) for all scenarios considered.

We assign these to be virtually certain to very likely (defined as agreement among most models, or, where only a small number of models have been analyzed and their results are physically plausible, these have been assessed to characterize those from a larger number of models). The more recent results are generally obtained from models with improved parameterizations (e.g., better land-surface process schemes).

a) The troposphere warms, stratosphere cools, and near surface temperature warms.

b) Generally, the land warms faster than the ocean, the land warms more than the ocean after forcing stabilizes, and there is greater relative warming at high latitudes.

c) The cooling effect of aerosols from troposphere moderates warming both globally and locally, which mitigates the increase in SAT.

d) The SAT increase is smaller in the North Atlantic and circum-polar Southern Ocean regions relative to the global mean.

e) As the climate warms, Northern Hemisphere snow cover and sea-ice extent decrease.

f) The globally averaged mean water vapor, evaporation and precipitation increase.

g) Most tropical areas have increased mean precipitation, most of the sub-tropical areas have decreased mean precipitation, and in the high latitudes the mean precipitation increases.

h) Intensity of rainfall events increases.

i) There is a general drying of the mid-continental areas during summer (decreases in soil moisture). This is ascribed to a combination of increased temperature and potential evaporation that is not balanced by increases in precipitation.

j) A majority of models show a mean El Niño-like response in the tropical Pacific, with the central and eastern equatorial Pacific sea surface temperatures warming more than the western equatorial Pacific, with a corresponding mean eastward shift of precipitation.

k) Available studies indicate enhanced inter-yearly variability of northern summer monsoon precipitation.

Received, June 4, 2008

Technical University "Gheorghe Asachi", Jassy,
Department of Hydrotechnical Structures and
Sanitary Engineering

REFERENCES

1. Antohi C., *Monitoring of Environmental Factors (in Romanian),* ed. Performantica, 2005, Iasi;
2. Bhaskharan B., Mitchell J.F.B., 1998: *Simulated changes in the intensity and variability of the southeast Asian Monsoon in the Twenty first Century Resulting from Anthropogenic Emissions Scenarios. Int. J. Climatol,(1998)*
3. Brinkop, S.,*Change of Convective Activity and Extreme Events in a Transient climate change Simulation, DLR-Insti. fur Physik der Atmosphaere, Report* No. 142(2001)
4. Giurma I., *Special Hydrology (in Romanian),* Ed. Politehnium, 2004, Iasi
5. Gregory, J.M. and J.F.B. Mitchell, *The climate response to CO2 of the Hadley Centre coupled AOGCM with and without flux adjustment.* Geophys. Res. Lett., 24, 1943-1946. (1997)
6. Gregory, J.M., J.F.B. Mitchell A.J. Brady: *Summer Drought in Northern Mid-latitudes in a Time-dependent CO2 climate experiment.* J. Climate, 10(1997)
7. Hennessy, K.J., J.M. Gregory and J.F.B. Mitchell, *Changes in Daily Precipitation under Enhanced Greenhouse Conditions: Comparison of UKHI and CSIRO9 GCM.* Clim. Dyn., 13, 667-680. (1997)
8. Kharin, V.V. and F.W. Zwiers: *Changes in the Extremes in an Ensemble of Transient Climate Simulations with a Coupled Atmosphere-Ocean* GCM. J. Climate, (2000)
9. Kothavala, Z.: *Extreme precipitation events and the applicability of global climate models to study floods and droughts.* Math. and Comp. in Simulation, 43, (1997)
10. Meehl, G.A., G.J. Boer, C. Covey, M. Latif and R.J. Stouffer, 2000: *The Coupled Model Intercomparison Project (CMIP).* Bull. Am. Met. Soc.
11. Sankovski A., M. Schlesinger, P. Shukla, S. Smith, R. Swart, S. van Rooijen, N. Victor, Z. Dadi: IPCC Special Report on Emissions Scenarios, Cambridge University Press, Cambridge, United Kingdom and New York, NY, USA, (2000)
12. Zwiers, F.W. and V. V. Kharin: Changes in the Extremes of the Climate Simulated by CCC GCM2 under CO2-doubling. *J. Climate*, 11(1998)

ANALIZA PERSPECTIVELOR SCHIMBARILOR CLIMATICE UTILIZAND MODELAREA MATEMATICA

(Rezumat)

Scopul lucrarii este de a analiza si cuantifica proiectii ale posibilelor schimbari climatice rezultate din diferite modele climatice. Sunt analizate variate posibilitati precum si posibilele raspunsuri sub presiunea factorilor de mediu care afecteaza variatiile climei.

BULETINUL INSTITUTULUI POLITEHNIC DIN IAŞI
Publicat de
Universitatea Tehnică „Gheorghe Asachi” din Iaşi
Tomul LIV (LVIII), Fasc. 2, 2008
Secţia
HIDROTEHNICĂ

SLOPE STABILITY STUDY BASED ON GIS ALGORITHM

BY

MAGYARI-SÁSKA ZSOLT and HAIDU IONEL

Based on the SINMAP model our study presents the implementation and development of an ArcGIS macro for determining the most probable trigger points of landslides.

Key words: SINAMP model, trigger points, algorithm implementation, Mures Basin, ArcGIS macro

1. Introduction - the SINMAP model

The study of a phenomenon can be made on quantitative or qualitative manner, using direct or indirect methods. The indirect methods based on GIS are used especially for larger areas [1]. For studying slope stability the data driven or process driven methods are both convenient, but in case of historical data lack the last methodology is suitable. The infinite slope model is used on SHALSTAB [2] and SINMAP submodels. While SHALSTAB neglects the root cohesion [3] SINMAP takes account also this aspect. The SINMAP stability index used to study the phenomenon is determined on the basis of the following formula:

$$SI = \frac{C + \cos\theta(1 - wr)\tan\phi}{\sin\theta}$$

where,

$$C = \frac{C_s + C_r}{h\rho_s g} \qquad w = \frac{h_w}{h} \qquad r = \frac{\rho_w}{\rho_s}$$

C_s - force of soil cohesion
C_r - roots cohesive force
ρ_w - density of water
ρ_s - density of soil
h - coating soil thick
h_w - water layer thick of the soil
θ - region slope
φ - friction angle

One of the advantages of the method is that the value of index is categorized into the meanings what it defines. Another advantage is that for some parameters is possible to define a value frame, through removing the necessity of time costing exact measurements. Another advantage is that for the analysis is not necessarily to have a historical database of landslides.

Table 1.
The appreciation of the value index of stability

SI value	Stability	Influences
>1.50	Stable	Instability may occur due to major factors of destabilization
1.50 – 1.25	Moderately stable	Instability may occur due to medium factors of destabilization
1.25 – 1.00	Slightly stable	Instability may occur due to minor factors of destabilization
1.00 – 0.50	Lower threshold of instability	Instability without external factors
0.50 – 0.00	Higher threshold of instability	The stability is due to the presence of stabilization factors
<0.00	Instable	Stabilization factors are required

Interpreting the sense of stability factor (Table 1) as the ratio between the forces who oppose to landslide and those favoring sliding, when the value factor is above 1, the area can be considered stable.

2. Case study – the SINMAP extension and the necessary data

Although there are several possibilities for the study the chosen method was SINMAP for several reasons. Firstly the results provided by this methodology are directly interpretable, and may constitute inputs for a possible further analysis, and secondly the existence of a program (ArcView/ArcGIS extension) allows an easy approach to the analysis.

SINMAP extension is freely available in two variants for ArcGIS and ArcView respectively (figure 1). The possibilities offered not differ significantly, and neither the way of calculation.

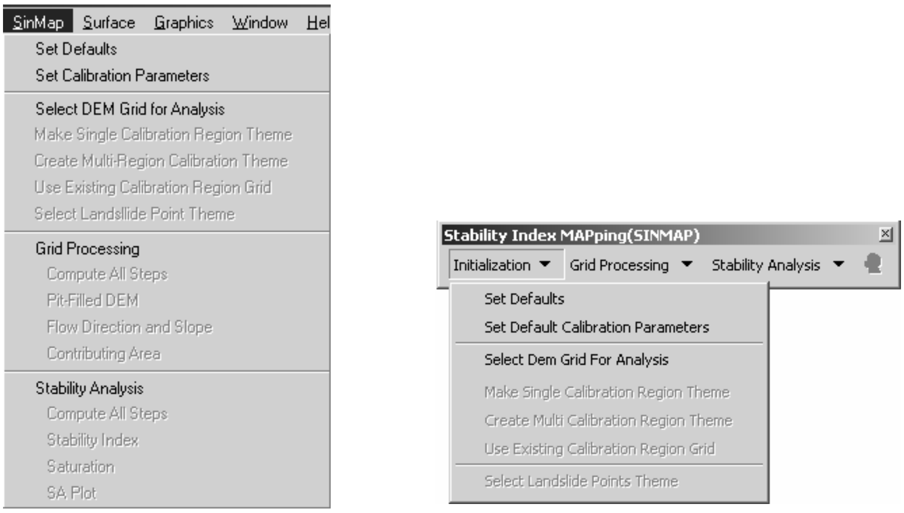

Fig. 1. Interface of SINMAP extension in ArcView 3. 2 and ArcGIS 9. 2

The performed steps of the analysis using these extensions are:

- the selection of digital elevation model
- the decision on the type of study areas (zone unit or multi-zone)
- defining the parameters for each area of analysis
- the removal of imperfections of elevation model
- calculating the slope and drainage maps
- determining the drainage areas
- calculating the stability map

It’s not necessary to include the rock type in the study as the SINAMP model doesn’t models rock falls, just landslide. [4]

Steps remembered are absolutely necessary to carry out the study regarding the slope stability. However the system offers other possibilities, such as specifying the location recorded landslides.

The SINAMP extension comply with the idea of automatic spatial analysis, since-as after defining the entry parameters with two mouse clicks the whole analysis is carried out automatically, thus allowing the rerun of the full analysis (and possibly reuse partial results which are not amended - ex. slopes map) with different parameters.

Parameters relating to the properties of the soil in the area were approximate with values of similar studies and soil tables [5].

Based on the calculation formula of stability index the cohesion is without measure, since-as they relate to the product of density, gravity acceleration and soil depth. Also the cohesion should contain the root cohesion.

For this latter amount initially a range between 0-5 kPa was considered.

Another requested parameter of the SINMAP model is the T/R report, where T is soil transmissivity and R is the rate of ground recharging for a short period, preferably before the landslide. Transmissivity can be calculated based on hydraulic conductivity and soil thickness, as follows:

$$T = k_s \cdot H$$

Based on tables the hydraulic conductivity varies between 0001 and 0.000001 cm/s depending on the composition of the soil.

For an approximation of the ground recharging value there are several options. When we have historical records on landslides a possibility is to use the values of precipitation before the sliding period [6]. Without these records another possibility would be to use the value of the maximum daily precipitation [7]. In the present analysis, having no historical records on landslides, but taking account that the phenomenon occurs due to soil saturation, having direct link with abundant rainfall, has used the following methodology for assessing the recharging value:

- interpolating the precipitation recorded at meteorological stations in the area based on the study of multiple regression

- determining the percent of minimum and maximum daily precipitation over annual rainfall taking account all meteorological stations

- for each study zone (determined based on the soil type) the average interpolated precipitation is calculated

- based on the percents determined in the previous step to determine the two limits (minimum and maximum) of recharge value (R) is calculated

A relatively recent [8] research makes further analysis seeking those points at which is most likely the launch of landslide can appear. The trigger besides that must have a classification of instability based on SINMAP analysis must be along the drain canal.

To determine these points in a GIS system, Tarolli proposes the following principle:

- determining the minimum values of stability index along the drainage channels with downstream spreading
- determining the minimum values of stability index along the drainage channels with upstream spreading
- those cells that have equal stability index under a certain fixed threshold, are the most vulnerable points where they can trigger the landslides.

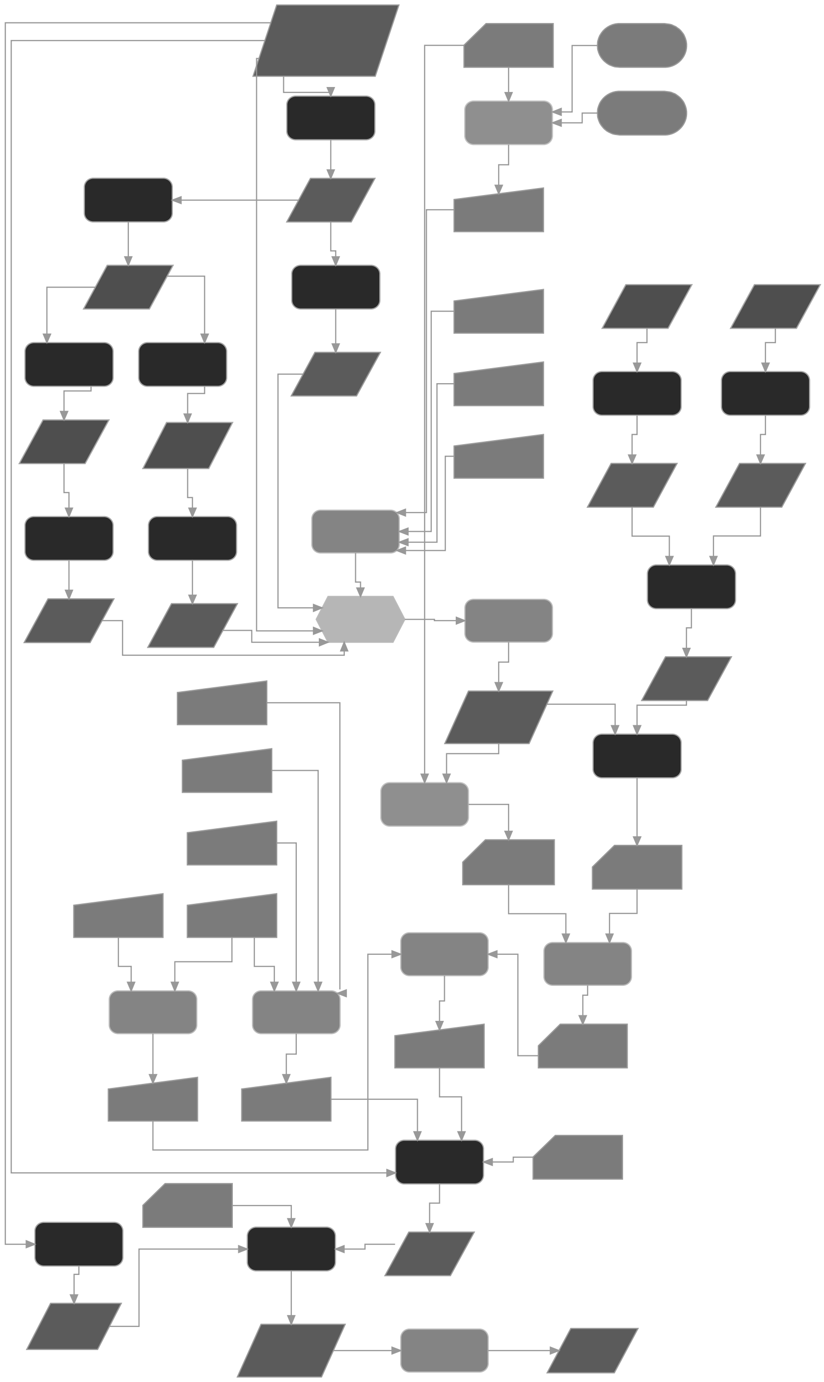

Fig. 2. The algorithm used in the study of slope stability

Tarolli noted that the algorithm was implemented in C programming language, in a recurring way. Given that, recursivity is a programming method that require significant resources of calculation (memory capacity and calculation power) and that any approach to a recursive problem has an iterative solution, the study proposes to develop a not recursive implementation of the basic algorithm, using the statistical system in R and Borland Delphi [9].

The two raster layers containing the propagated stability index in both directions (downstream and upstream) boots with the original stability index.

Knowing that the flow directions in ArcGIS are represented by a direction matrix a symmetrical one has been made, so that the direction from which water flows in the middle cell can be identified.

Matrix thus obtained is situated on each cell in the image representing low directions, and the where values of the image coincide with the mask there the minimum value for the index of stability was chosen. This way the downstream spread of stability index value is made.

With the downstream spread the upstream spreading is done, generating the corresponding image using the same mask. In this case, however, if the current cell contains a lower stability index than the center cell this is propagated to those cells whose flow directions coincide with the directions under the mask.

The overlap of the mask is repeated until there is at least one cell value change in any direction, after which another function, for which must be specified the threshold value of instability, marks those cells that are below the threshold values and present equal values to the index of stability.

3. Results and discussion

The methodology has been applied to the study region. In some areas the obtained results confirms the reality (Gheorgheni Lăzarea, Gălăuţaşi), but there are areas in which the danger of instability seems exaggerated and inconclusive. We also should note the fact that there are no areas with extremely dangerous slide imminent (upper threshold).

Trying to obtain a conclusive result we considered the vegetation on Corine Land Cover 2000, making a crosstabulation of two levels one with the content of clay, with the various coverings of vegetation. Four classes have been defined for vegetation coverage (lack of vegetation, agricultural crops, poor vegetation, forest area), for each giving the values of cohesion due roots.

The result obtained is more eloquent (figure 3). On the one hand it is noted a much clearer appreciation of dangerous areas, and the cells with high risk appears, particularly in the area of Sălard and Gălăuţaşi. It is considered as danger zones the lower river of and downstream of the lake Răstoliţa. The most likely trigger points are offered after running the own developed module (figure 4).

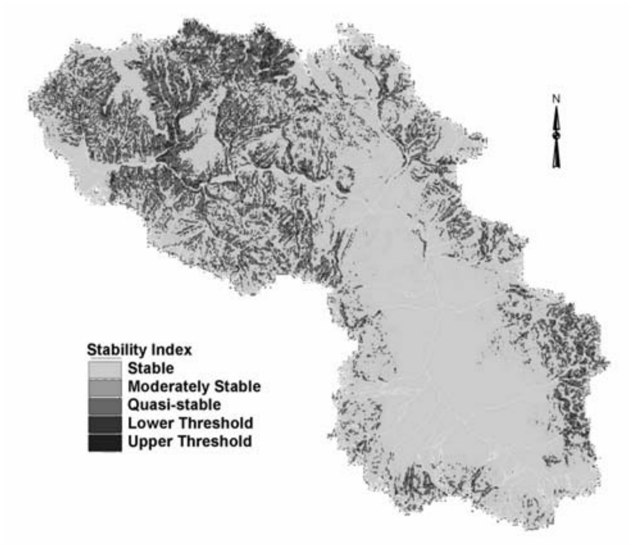

Fig. 3. Index stability map, taking account the land use

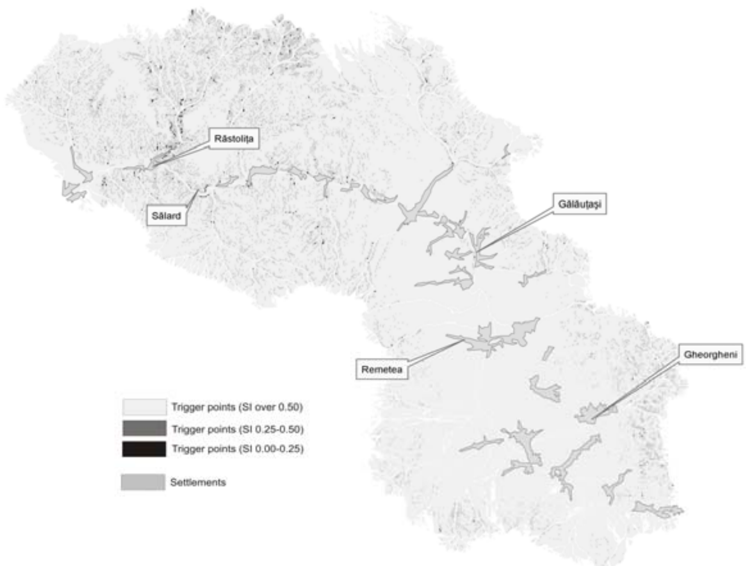

Fig. 4. The most likely trigger points of landslides

Taking account the probabilistic interpretation of stability index stability (values over 1 represents stable areas, and values below 1 the probability that in the specified location landslides will not occur), but also the method how to account values below 1 (using cumulative probability functions) the transformation of these probabilities has been made in return periods.

This transformation has been achieved for both the stability index map obtained from the SINMAP analysis and for the map containing the most likely trigger locations for landslides.

4. Conclusions

The research includes both methodological and practical aspect. Even if the base methodology for determining the SINMAP stability index is given, the calibration of most of its parameters is difficult. The possibility of SINMAP model to define parameter intervals is a great advantage is such cases. The importance of root cohesion (neglected in SHALSTAB model) is clearly revealed, because without it the stability index map doesn't presents obvious values.

The free R statistical system presents handicap when we want to operate on huge matrix structures, its calculating speed doesn't permit a useful integration in an ArcGIS macro, so we have to implement the Tarolli's algorithm in a general programming language. Even with this remark the possibility to integrate different programming environments in ArcGIS permits that special operations which are strongly related to a GIS algorithm (ex. statistical work), but are not implemented in such systems could be performed by specialized applications.

R E F E R E N C E S

1. C a r r a r a A., C a r d i n a l i M., G u z z e t t i F., R e i c h e n b a c h P., *GIS technology in mapping landslide hazard*, *Geographical Information Systems in Assessing Natural Hazards*. Kluwer Academic Publisher, Dordrecht, The Netherlands, 135-175 (1995)

2. D i e t r i c h W. E., M o n t g o m e r y D. R., *SHALSTAB, A digital terrain model for mapping shallow landslide potential*, Technical report, NCASI, http://socrates.berkeley.edu/~geomorph/shalstab/, (1998)

3. G u i m a r ã e s R.F., R a m o s V.M., R e d i v o A.L., G o m e s R.A.T., F e r n a n d e s N.F., d e C a r v a l h o O.A., *Application of the SHALSTAB Model for Mapping Susceptible Landslide Areas in Mine Zone* (Quadrilátero Ferrífero in Southeast Brazil), Geoscience and Remote Sensing Symposium, 2003. IGARSS '03. Proceedings. 2003 IEEE International Volume 4, 2444-2446 (2003)

4. P a c k R.T., T a r b o t o n D.G., G o o d w i n C.N., , *Assessing Terrain Stability in a GIS using SINMAP*, *15th annual GIS conference*, GIS 2001, February 19-22, Vancouver, British Columbia, (2001)

5. W a w e r R., N o w o c i e ń E., *Application of SINMAP terrain stability model to Grodarz stream watershed*, Electronic Journal of Polish Agricultural Universities, Vol. 6, Issue 1, (2003)

6. W e e r a s I n g h e K.M., A b e y w I c k r e m a H.V.M.P., F o w z e J.S.M., S a m a r a k o o n L., *Use of a deterministic slope stability predicting toll for landslide vulnerability assessment in Ratnapura area, Sri Lanka, International conference on Mitigation of the Risk of Natural Hazards*, Peradeniya, Sri Lanka, 27-28 March 2007, (2007)

7. U d a s A., *Slope stability analysis using GIS on a regional scale: a case study of Narayanghat – Mungling highway section, Nepal*, Master Dissertation, Universiteit Gent Vrije Universiteit Brussel, Belgium, (2005)

8. T a r o l l i P., T a r b o t o n D. G., *A new method for determination of most likely landslide initiation points and the evaluation of digital terrain model scale in terrain stability mapping*, Hydrology and Earth Science System, 10, 663-677, (2006)

9. M a g y a r i – S á s k a Zs., H a i d u I., *Possibilities of spatial modeling in programmed environments (Posibilităţi de modelare spaţială în mediu programat)*, Scientific Journal of „Al. I. Cuza" University, Iaşi, Geography, LII, 57-65 (2006)

Received, November 25, 2008

Babes-Bolyai University, Faculty of Geography

STUDIUL STABILITĂŢII VERSANŢILOR BAZAT PE ALGORITM GIS

(Rezumat)

Pentru studiu stabilităţii versanţilor există mai multe posibilităţi, unele se bazează pe abordare statistică, altele pe modelarea fenomenului. Modelul pantei infinite stă la baza modelelor SHALSTAB şi SINMAP, care utilizează cea de a doua abordare. Modelul SINMAP este implementat ca şi extensii pentru sistemele ArcView şi ArcGIS, având avantajul dea utiliza calcul probabilistic pentru aprecierea stabilităţii. Studiul prezentat realizează o calibrare a parametrilor modelului SINMAP pentru Bazinul Superior al Mureşului, ţinând cont şi de coeziune solului datorată vegetaţiei, după care – pe baza unei extensii ArcGIS de dezvoltare proprie – determină cele mai probabile puncte de declanşare a alunecărilor, folosind atât harta indicelui de stabilitate cât şi harta direcţiilor de scurgere, conform algoritmului lui Tarolli. Pe baza rezultatelor se observă că locaţiile cu cel mai mare grad de periculozitate se află în special în zona localităţii Sălard şi Gălăuţaşi. Este considerată zonă periculoasă şi cursul inferior a râului Răstoliţa în aval de lacul Răstoliţa.

BULETINUL INSTITUTULUI POLITEHNIC DIN IAŞI
Publicat de
Universitatea Tehnică „Gheorghe Asachi” din Iaşi
Tomul LIV (LVIII), Fasc. 2, 2008
Secţia
HIDROTEHNICĂ

MODELLING OF A HYDROPHORE PUMPING FACILITY IN SLOW VARIABLE OPERATIONAL REGIMES

BY

POPESCU ŞTEFAN, MARCOIE NICOLAE and TOMA DANIEL

The paper presents the conceptual and mathematical models which are describing the functioning of a hydrophore pumping facility, working in quasi-permanent and slow-variable transition regimes. This modelling, achieved within the systems’ theory, serves to compute the main power and economic efficiency parameters of water pumping, and those for pumps’ starting and stopping sequences.
Key words: modelling, hydrophore, efficiency

1. Introduction

One frequently used way to adapt pumps to the variable demands of water supply networks is the intermitent operation of non-adjustable pumps and the hydrophore based compensation of flows. If such facilities are soundly designed and operated they can adequately satisfy the network’s demands in terms of flows and loads, they can provide a decrease of the pump’s starting sequnces’ frequency and they can ensure the network’s protection against surge damages.

Below we present the modelling of a hydrophore pumping facility, in quasi-permanent and also in slow-variable transition operating regimes.

2. Conceptual model

The considered hydrophore pumping facility draws water from a suction tank (vessel), having a free constant level, and delivers it directly towards a pressurized water supply network. This network’s flow and load demands are constant during the analysis (study) period. The pumping basic technological line (PBTL) is equipped with $N_{tip} \leq 2$ non-adjustable pumping devices (PD), as it follows: $m_p^{I} > 0$ - main PD şi $m_p^{II} \geq 0$ - auxiliary PD; the $m_p^{I} + m_p^{II}$ PD can work in parallel and are constituted in the so-called [3, 4] *hydraulic generators battery* (HGB).

A variant of functioning for the HGB, ν, is described via the number of PD of each type, in function, $(\overline{m}_p^{I}, \overline{m}_p^{II})$, where $0 \leq \overline{m}_p^{I} \leq m_p^{I}$ and $0 \leq \overline{m}_p^{II} \leq m_p^{II}$. The total number of HGB's operational variants, N_v (inclusding the variant $\overline{m}_p^{I} = \overline{m}_p^{II} = 0$), is $N_\nu = (m_p^{I} + 1)\,(m_p^{II} + 1)$.

The hydraulical system represented by PBTL and hydrophore, schematically, features N_{sc}=3 characteristical sections (Fig. 1), namely: *k*=1 – via HGB's delivery collector; *k*=2 – via the common delivery pipe's connection with hydrophore R_2, considered to be cylindrical, with a horizontal generator (Fig. 2); *k*=3 – via the delivery pipe's connection that is connecting it to the served water supply network. Depending on served water network's needs and the PD's functional parameters, this hydraulic system can operate in a continuous way (quasi-permanentregime) or in a discontinuous way (slow variable transition regime).

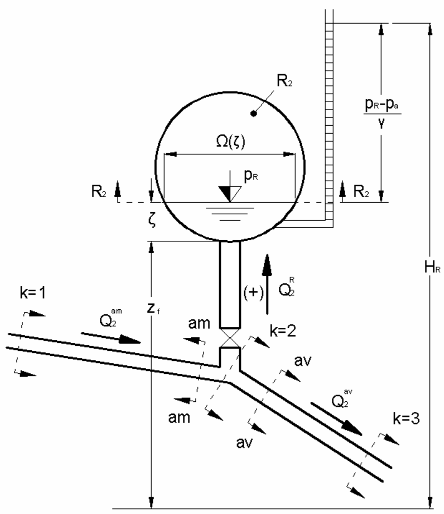

Fig.1. Diagram of hydraulic system PBTL-hydrophore

Considering its functions, according to [1], in a hydrophore having a total volume V_H, the next characteristical volumes can be described (Fig. 2):

A water volume needed to prevent the weakening of air cushion, V_o; An anti-surge volume, V_p ; A volume available for flow compensation, V_u , and the volume of compressed air, V_a , required vor providing the load in the tank, H_2^R .

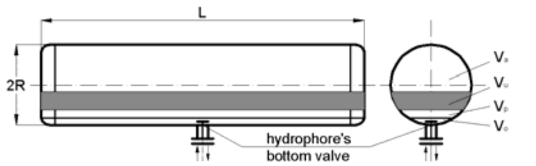

Fig.2. Geometrical features of a horizontal cylindrical hydrophore

3. Mathematical model

The conceived mathematical model is based on the laws which govern the transformation of compressed air volume within the hydrophore, the way in which HGB works together with the water supply network, and, as well, the way in which the generating hydraulic machine works together with the electric driving motor, from a mechanical point of view.

In order to fully satisfy at least the water supply network's demands, the piezometrical loads within section $k = 2$, $\mathrm{H}_2^{\mathrm{am}}(t)$, in delivery collector, $\mathrm{H_C}(t)$, and within compensation tank, $\mathrm{H_R}(t) = z_f + \zeta(t)$, have to satisfy the following restrictions:

$$\mathrm{H_C}(t) \geq \mathrm{H}_2^{\mathrm{am}}(t) \geq H_{\mathrm{F}} \quad ; \quad H_{\mathrm{R}}^{\min} \leq \mathrm{H_R}(t) \leq H_{\mathrm{R}}^{\max} \quad ; \quad H_{\mathrm{F}} \leq \mathrm{H}_2^{\mathrm{av}}(t) \leq H_{\mathrm{R}}^{\min} . \tag{2}$$

For the situation $\mathrm{H}_3^{\mathrm{av}}(t) \equiv \mathrm{H_F}(t) = H_{\mathrm{F}}^{\min}$, variants ν , $(\nu = 1,2,\cdots,N_\nu)$, are to be ordered in an augmenting manner function of the HGB's flow, Q_ν ; therefore the next inequalities are satisfied:

$$0 \leq Q_\nu < Q_{\nu+1} \quad , (\forall)\ \nu \in \{1,\cdots,N_\nu - 1\} . \tag{3}$$

In case of *continuous functioning* there is at least one variant ν^* , $\nu^* \in \{1,2,\cdots,N_\nu\}$, for which relations below are verified:

$$Q_{\nu^*} = Q_{\mathrm{F}} \ , \text{ cu } \quad H_{\mathrm{R}}^{\min} \leq \mathrm{H}_2^{\mathrm{am}}(t) \leq H_{\mathrm{R}}^{\max} . \tag{4}$$

The pumping facility with compensation tank works *in a cyclic manner* when there is a HGB's functioning variant ν^* , $\nu^* \in \{2,\cdots,N_\nu\}$, in order to simultanously satisfy the next conditions:

$$\mathrm{H}_2^{\mathrm{am}}(t) > H_{\mathrm{R}}^{\max} \text{ , pentru } \quad Q_{\nu^*} = Q_{\mathrm{F}} \text{ ;} \tag{5}$$

$$\mathrm{H}_2^{\mathrm{am}}(t) < H_{\mathrm{R}}^{\min} \text{ , pentru } \quad Q_{\nu^*-1} = Q_{\mathrm{F}} \text{ .} \tag{6}$$

In this case we can describe the next: 1^0 - the compensation tank's filling stage and 2^0 - the compensation tank's draining stage.

During the filling stage, with duration T_{u} , HGB works in the variant ν^*, and the H_{R} load increases from initial value $H_{\mathrm{R}}^{\min}$ to final value $H_{\mathrm{R}}^{\max}$.

During the draining stage, with duration T_{g} , HGB works in variant ν^* - 1, and the piezometrical load H_{R} is decreasing from initial value $H_{\mathrm{R}}^{\max}$ to final value $H_{\mathrm{R}}^{\min}$.

Obviously, for the whole cycle's duration, it results:

$$T = T_{\mathrm{u}} + T_{\mathrm{g}} \text{ .} \tag{7}$$

Next we will present, classified in groups with remarkable technical meanings, firstly the computing equations needed to model the pumping facility for a continous regime (quasi-permanent), and next the additional and/or specific equations (corresponding to a variable slow transition regime) , which occur in the case of cyclic functioning.

3.1. Mathematical model in case of continuous functioning

This model is described by means of equations given at items a)...l).

a) *Pump's characteristics at variable speed* [3, 4]:

- for load,

$$\mathrm{H}^i\left(Q_{\mathrm{p}}^i, n^i\right) = a_H^i \cdot \left(n^i\right)^2 + b_H^i \cdot Q_{\mathrm{p}}^i \cdot n^i + c_H^i \cdot \left(Q_{\mathrm{p}}^i\right)^2 \quad , \quad i \in \{\mathrm{I}, \mathrm{II}\} \text{ ;} \tag{8}$$

- for power,

$$\mathrm{N}^i\left(Q_{\mathrm{p}}^i, n^i\right) = a_N^i \cdot \left(Q_{\mathrm{p}}^i\right)^2 \cdot n^i + b_N^i \cdot Q_{\mathrm{p}}^i \cdot \left(n^i\right)^2 + c_N^i \cdot n^i + d_N^i \cdot \left(n^i\right)^3 \text{ , } \quad i \in \{\mathrm{I}, \mathrm{II}\} \text{ ;} \tag{9}$$

- for torque,

$$\mathcal{M}^i\left(Q_{\mathrm{p}}^i, n^i\right) = a_{\mathcal{M}}^i \cdot \left(Q_{\mathrm{p}}^i\right)^2 + b_{\mathcal{M}}^i \cdot Q_{\mathrm{p}}^i \cdot n^i + c_{\mathcal{M}}^i + \cdot d_{\mathcal{M}}^i \cdot \left(n^i\right)^2 \text{ , } \quad i \in \{\mathrm{I}, \mathrm{II}\} \text{ .} \tag{10}$$

b) *Asynchron motor's characteristics* [3, 4]:

- for torque,

$$\mathcal{M}_{\mathrm{m}}^i\left(n^i\right) = \frac{a_1^i\left(n_s^i - n^i\right)}{\left(n^i\right)^2 + b_1^i \cdot n^i + c_1^i} \quad , \quad i \in \{\mathrm{I}, \mathrm{II}\} \text{ ;} \tag{11}$$

- for power factor,

$$\cos\varphi^{i}\left(\mathcal{M}_{\mathrm{m}}^{i}\right)=a_{\varphi}^{i}\cdot\left(\mathcal{M}_{\mathrm{m}}^{i}\right)^{2}+b_{\varphi}^{i}\cdot\mathcal{M}_{\mathrm{m}}^{i}+c_{\varphi}^{i}\,,\quad cu\quad i\in\{\mathrm{I},\mathrm{II}\}\;; \qquad (12)$$

- for cost efficiency,

$$\eta_{1}^{\prime i}\left(n^{i},\mathcal{M}_{\mathrm{m}}^{i},\varphi^{i}\right)=\frac{1}{1+\tilde{\rho}\cdot\left(\mathrm{tg}\varphi^{i}-\mathrm{tg}\varphi_{\mathrm{ne}}\right)}\cdot\frac{n^{i}\cdot\mathcal{M}_{\mathrm{m}}^{i}}{\tilde{e}^{i}\cdot\left(\mathcal{M}_{\mathrm{m}}^{i}\right)^{2}\cdot\left(n^{i}\right)^{2}+\mathcal{M}_{\mathrm{m}}^{i}\cdot n^{i}+\tilde{f}^{i}}\,,$$

$$cu\quad i\in\{\mathrm{I},\mathrm{II}\}\,, \qquad (13)$$

c) The water network's equivalent characteristic (NEC),
(against section $k = 3$) [3]:

$$\mathrm{H}_{3}\left(Q_{\mathrm{F}}\right)=H_{\mathrm{ech}}^{\mathrm{st}}+M_{\mathrm{ech}}\cdot\left(Q_{\mathrm{F}}\right)^{p}\,, \qquad (14)$$

d) *Energy equations*:

- between sections k=1 *and* k=2,

$$\mathrm{H}_{2}^{\mathrm{am}}(t)=\mathrm{H}_{\mathrm{C}}(t)-\mathrm{h}_{\mathrm{r}}^{1,2}\left(Q_{1}^{av}\right), \qquad (15)$$

- between sections k=2 and k=3,

$$\mathrm{H}_{3}^{\mathrm{am}}(t)=\mathrm{H}_{2}^{\mathrm{av}}(t)-\mathrm{h}_{\mathrm{r}}^{2,3}\left(\mathrm{Q}_{2}^{\mathrm{av}}(t)\right), \qquad (16)$$

Applying technique given in [4] , from equations (8) ÷ (11), the next elements have been computed:

e) *Pumps' characteristics ,*
at quasi-constant speed:

- for load

$$\overline{\mathrm{H}}^{i}\left(Q_{\mathrm{p}}^{i}\right)=\overline{a}_{H}^{i}+\overline{b}_{H}^{i}\cdot Q_{\mathrm{p}}^{i}+\overline{c}_{H}^{i}\cdot\left(Q_{\mathrm{p}}^{i}\right)^{2},\quad i\in\{\mathrm{I},\mathrm{II}\}\,; \qquad (17)$$

- for power

$$\overline{N}^{i}\left(Q_{\mathrm{p}}^{i}\right)=\overline{a}_{N}^{i}+\overline{b}_{N}^{i}\cdot Q_{\mathrm{p}}^{i}+\overline{c}_{N}^{i}\cdot\left(Q_{\mathrm{p}}^{i}\right)^{2},\quad i\in\{\mathrm{I},\mathrm{II}\}\,; \qquad (18)$$

- for torque

$$\overline{\mathcal{M}}^{i}\left(Q_{\mathrm{p}}^{i}\right)=\overline{a}_{\mathcal{M}}^{i}+\overline{b}_{\mathcal{M}}^{i}\cdot Q_{\mathrm{p}}^{i}+\overline{c}_{\mathcal{M}}^{i}\cdot\left(Q_{\mathrm{p}}^{i}\right)^{2},\quad i\in\{I,II\}\,; \qquad (19)$$

- the speed's variation laws,

$$\overline{\mathrm{n}}^{i}\left(Q_{\mathrm{p}}^{i}\right)=\overline{a}_{n}^{i}+\overline{b}_{n}^{i}\cdot Q_{\mathrm{p}}^{i}+\overline{c}_{n}^{i}\cdot\left(Q_{\mathrm{p}}^{i}\right)^{2},\quad i\in\{\mathrm{I},\mathrm{II}\}\,. \qquad (20)$$

f) *The reduced load characteristics (in delivery collector's section) :*

$$\overline{\mathrm{H}}'^{i}\left(Q_{\mathrm{p}}^{i}\right)=\overline{a}_{H}^{i}+\overline{b}_{H}^{i}\cdot Q_{\mathrm{p}}^{i}+\overline{c}'^{i}_{H}\cdot\left(Q_{\mathrm{p}}^{i}\right)^{2},\quad i\in\left\{\mathrm{I},\mathrm{II}\right\}; \tag{21}$$

g) *HGB's equivalent load characteristic*:

- <u>for variant ν</u>, which gives $\overline{m}_{\mathrm{p}}^{i}\neq 0$ şi $\overline{m}_{\mathrm{p}}^{j}=0$, $cu\ (i,j)\in\left\{\mathrm{I},\mathrm{II}\right\}$ şi $i\neq j$:

$$\overline{\mathrm{H}}(\nu,Q)=\overline{a}_{H}^{i}+\frac{\overline{b}_{H}^{i}}{\overline{m}_{\mathrm{p}}^{i}}\cdot Q+\frac{\overline{c}'^{i}_{H}}{\left(\overline{m}_{\mathrm{p}}^{i}\right)^{2}}\cdot Q^{2}, \tag{22}$$

- <u>for variant ν</u>, which gives $\overline{m}_{\mathrm{p}}^{\mathrm{I}}\geq 1$ şi $\overline{m}_{\mathrm{p}}^{\mathrm{II}}\geq 1$:

$$\overline{\mathrm{H}}(\nu,Q)=b_{H}+c_{H}\cdot\left(Q-a_{H}\right)^{2}+d_{H}\cdot\left(Q-a_{H}\right)\sqrt{\left(Q-a_{H}\right)^{2}+e_{H}}, \tag{23}$$

where:

$$a_{H}=-\frac{1}{2}\left(\overline{m}_{\mathrm{p}}^{I}\cdot\frac{\overline{b}_{H}^{\mathrm{I}}}{\overline{c}'^{\mathrm{I}}_{H}}+\overline{m}_{\mathrm{p}}^{\mathrm{II}}\cdot\frac{\overline{b}_{H}^{\mathrm{II}}}{\overline{c}'^{\mathrm{II}}_{H}}\right)\quad;\quad b_{H}=\frac{\left(\alpha^{\mathrm{I}}\right)^{2}\beta^{\mathrm{I}}-\left(\alpha^{\mathrm{II}}\right)^{2}\beta^{\mathrm{II}}}{\gamma}\quad;$$

$$c_{H}=-\frac{\left(\alpha^{\mathrm{I}}\right)^{2}+\left(\alpha^{\mathrm{II}}\right)^{2}}{\gamma^{2}}\quad;\quad d_{H}=2\,\frac{\alpha^{\mathrm{I}}\alpha^{\mathrm{II}}}{\gamma^{2}}\quad;\quad e_{H}=\gamma\left(\beta^{\mathrm{II}}-\beta^{\mathrm{I}}\right) \tag{24}$$

And in which

$$\alpha^{i}=\frac{\overline{m}_{\mathrm{p}}^{i}}{\sqrt{-\overline{c}'^{i}_{H}}};\ \beta^{i}=\overline{a}_{H}^{i}-\frac{\left(\overline{b}_{H}^{i}\right)^{2}}{4\overline{c}'^{i}_{H}},\ \text{cu}\ i\in\left\{\mathrm{I},\mathrm{II}\right\}\ \text{şi}\ \gamma=\left(\alpha^{\mathrm{I}}\right)^{2}-\left(\alpha^{\mathrm{II}}\right)^{2}; \tag{25}$$

h) *Energy's equations between the sections of suction tank and those of delivery collector:*

- for each pump,

$$H_{\mathrm{C}}=H_{\mathrm{A}}+\overline{\mathrm{H}}'^{i}\left(Q_{\mathrm{p}}^{i}\right),\quad cu\quad i\in\left\{\mathrm{I},\mathrm{II}\right\}; \tag{26}$$

- for HGB,

$$H_{\mathrm{C}}=H_{\mathrm{A}}+\overline{\mathrm{H}}(\nu,Q). \tag{27}$$

i) *The outline conditions in section k=1:*

$$s=s_{1};\ \boldsymbol{u}_{1}^{\mathrm{T}}=\left\{\overline{m}_{\mathrm{p}}^{\mathrm{I}}(\nu),\overline{m}_{\mathrm{p}}^{\mathrm{II}}(\nu)\right\}. \tag{28}$$

j) *The outline conditions in section k=2*

$$\mathrm{H}_{2}^{\mathrm{am}}-z-p_{2}/g\rho=0 \tag{29}$$

$$\left|\begin{cases} p_2 \cdot V_a(\varsigma) = W_H \\ z = z_{\mathrm{f}} + \varsigma \equiv const. \end{cases}\right. \tag{30}$$

k) *The outline conditions in section k=3*

$$\mathrm{Q}_3^{\mathrm{av}}(t) = \mathrm{Q}_3^{\mathrm{am}}(t)\,, \mathrm{Q}_3^{\mathrm{av}}(t) = \varphi_Q^3(t)\,,\ \mathrm{H}_3^{\mathrm{am}}(t) - \mathrm{H}_3^{\mathrm{av}}(t) - \mathrm{h}_{\mathrm{r}3}^{\mathrm{am,av}}\left(Q_3^{\mathrm{av}}\right) = 0\ . \tag{31}$$

l) *The powers' and efficiencies' equations:*

- electric motors' electrical power,

$$P_{\mathrm{e}}^i = \overline{\mathrm{N}}^i\left(Q_{\mathrm{p}}^i\right) \Big/ \eta\,{}'^i_1\left(n^i, \mathcal{m}_{\mathrm{m}}^i, \varphi^i\right)\ ,\quad i \in \{\mathrm{I}, \mathrm{II}\}\ ; \tag{32}$$

- pumping facility's electrical power,

$$P_{\mathrm{eSP}} = \overline{m}_{\mathrm{p}}^{\mathrm{I}} \cdot P_{\mathrm{e}}^{\mathrm{I}} + \overline{m}_{\mathrm{p}}^{\mathrm{II}} \cdot P_{\mathrm{e}}^{\mathrm{II}}\ ; \tag{33}$$

- hydraulic power requested by pilot network,

$$P_{h\mathrm{RP}} = \rho\ g\ Q_{\mathrm{F}}\left(H_{\mathrm{F}} - H_{\mathrm{A}}\right)\,, \tag{34}$$

- pumping facility's efficiency (specific equation) ,

$$\eta_{\mathrm{SP}} = 100\,\frac{P_{\mathrm{hRP}}}{P_{\mathrm{eSP}}}\ [\%]\ . \tag{35}$$

3.2. Mathematical model for cyclic functioning

In this case, besides equations from item *3.1.* [minus equations (15) and (16) as well as (29) and (30)], we have to take into account the next equations and conditions:

m) *Energy's equation between sections k*=2 *and* R_2 *tank's section*

$$\mathrm{H}_{\mathrm{R}}(t) = \mathrm{H}_2^{\mathrm{am}}(t) - \mathrm{h}_{\mathrm{r}2}^{\mathrm{am,R}}\left(Q, \varphi_Q^3(t)\right)\ , \tag{36}$$

Where head loss $\mathrm{h}_{\mathrm{r}2}^{\mathrm{am,R}}\left(Q, \varphi_Q^3(t)\right)$ is given by equation:

$$\mathrm{h}_{\mathrm{r}2}^{\mathrm{am,R}}\left(Q, \varphi_Q^3(t)\right) = \begin{cases} M_{\mathrm{am,R}}^{\mathrm{d}}\left(Q - \varphi_Q^3(t)\right)^2,\ pentru\ Q - \varphi_Q^3(t) \geq 0\,; \\ -M_{\mathrm{am,R}}^{\mathrm{i}}\left(Q - \varphi_Q^3(t)\right)^2,\ pentru\ Q - \varphi_Q^3(t) < 0\,, \end{cases} \tag{37}$$

n) *The wave's dynamic equation within delivery pipe and the continuity equation for compensation tank* R_2 :

- wave's dynamic equation

$$\frac{\alpha_0}{g}\cdot\frac{L_{1-2}}{A^*}\cdot\frac{\mathrm{dQ}(t)}{\mathrm{d}t} = \overline{\mathrm{H}}(\nu, Q) - z_{\mathrm{f}} - \varsigma - \mathrm{h}_{\mathrm{r}}^{1,2}(Q) - \mathrm{h}_{\mathrm{r}2}^{\mathrm{am,R}}\left(Q - \varphi_Q^3(t)\right); \tag{38}$$

- continuity equation for tank R_2

$$\Omega(\zeta)\frac{\mathrm{d}\zeta}{\mathrm{d}t}=Q-\varphi_Q^3(t) \ . \tag{39}$$

o) *Terminal conditions for the integration of equations* (38) and (39) :

- for tank's filling stage:

$$t_u^0=0 \ , \ Q_u^0=\varphi_Q^3\left(t_u^0\right) \ , \tag{40}$$

$$t_u^0=0 \ , \zeta_u^0=\left(\zeta\right)_{\min}=H_R^{\min}-z_{\mathrm{f}} \quad \text{şi}$$

$$t_u^1=T_{\mathrm{u}} \ , \zeta_u^1=\left(\zeta\right)_{\max}=H_{\mathrm{R}}^{\max}-z_{\mathrm{f}} \ ; \tag{41}$$

- for tank's draining stage:

$$t_{\mathrm{g}}^0=T_{\mathrm{u}} \ , \ Q_{\mathrm{g}}^0=\varphi_Q^3\left(t_{\mathrm{g}}^0\right) \ , \tag{42}$$

$$t_{\mathrm{g}}^0=T_{\mathrm{u}} \ , \zeta_{\mathrm{g}}^0=\left(\zeta\right)_{\max}=H_{\mathrm{R}}^{\max}-z_{\mathrm{f}} \ , \ t_{\mathrm{g}}^1=T \ , \zeta_{\mathrm{g}}^1=\left(\zeta\right)_{\min}=H_{\mathrm{R}}^{\min}-z_{\mathrm{f}} \ . \tag{43}$$

p) *The equations for pumping facility's energies and average efficiency:*

- power consumed in tank's operational stage ϕ ,

$$E_{\mathrm{eSP}}^{\phi}=\int_{t_\phi^0}^{t_\phi^1}\mathrm{P}_{\mathrm{eSP}}^{\phi}(t)\,\mathrm{d}t \ , \tag{44}$$

Where:

ϕ = u - for filling stage; ϕ = g - for draining stage;

- power consumed in T cycle,

$$E_{\mathrm{eSP}}=E_{\mathrm{eSP}}^{\mathrm{u}}+E_{\mathrm{eSP}}^{\mathrm{g}} \ ; \tag{45}$$

- hydraulic energy demanded by network, in cycle T,

$$E_{\mathrm{hRP}}=\rho\ g\ Q_{\mathrm{F}}\left(H_{\mathrm{F}}-H_{\mathrm{A}}\right)T \ ; \tag{46}$$

- pumping facility's average efficiency,

$$\eta_{\mathrm{SP}}=100\,\frac{E_{\mathrm{hRP}}}{E_{\mathrm{eSP}}}\quad[\%] \ . \tag{47}$$

Air cushion's volume, V_a , can be assessed in function of the water volume within the vessel, V_w, as it follows:

$$V_a=V_H-V_w \text{ with } V_w=V_o+V_p+V_u \tag{48}$$

In the usual cases of horizontal hydrophores (Fig. 2), water volume V_w can be computed as a function of the total volume V_H and the depth of water within the vessel, ς , as it follows[1]:

$$V_w=V_w(\varsigma)=V_H\cdot\Phi(\varsigma/R)\cong V_H\cdot(A\cdot\varsigma/R+B),\ \text{cu } V_H=\pi R^2L \tag{49}$$

And A=0.60303 and B= - 0.10418 for $\varsigma/R\in[0.3,1.7]$.

The precise equation of function $V_w(\varsigma)$ is given in [2]:

$$V_w(\varsigma)=\frac{L}{2}\left[D^2\left(\frac{\pi}{2}-arctg\sqrt{\frac{D-\varsigma}{\varsigma}}\right)+(2\varsigma-D)\sqrt{\varsigma(D-\varsigma)}\right] \quad (50)$$

The water's extreme levels within hydrophore's tank, that is $\varsigma^{\min}$ and $\varsigma^{\max}$, have to correspond to the extreme loads within tank, that is $H_R^{\min}$ and, respectively, $H_R^{\max}$; these levels depend on characterisic volumes by means of the next equations:

$$\varsigma^{\min}=V_w^{-1}\left(V_o+V_p\right) \text{ şi } \varsigma^{\max}=V_w^{-1}\left(V_o+V_p+V_u^{\max}\right) \quad (51)$$

From the isothermic transformation law, applied to the air cushion, it results:

$$\left[V_H-\left(V_o+V_p\right)\right]\left[p_a+g\rho\left(H_R^{\min}-z_f-\varsigma^{\min}\right)\right]=$$
$$=\left[V_H-\left(V_o+V_p+V_u^{\max}\right)\right]\left[p_a+g\rho\left(H_R^{\max}-z_f-\varsigma^{\max}\right)\right]=W_H \quad (52)$$

4. Conclusions

The above shown mathematical model is useful for the next applications:

1. To assess the main energetical and efficiency parameters for the water pumping process, that is E_{eSP} and η_{SP}.
2. To assess the control levels for pumps' startings and stoppings, that is: $\varsigma^{\min}$ / $\varsigma^{\max}$.
3. To create a computer program for the digital simulation of pumps' functioning.

REFERENCES

1. Alexandrescu O., *Staţii de pompare*. Ed. *Gh. Asachi* Iaşi, 2003, ISBN 973-621-059-6.
2. Bartha I., Luca M., Popescu Şt., Popia A. *Hidraulica. Culegere de probleme.* I.P. "Gh. Asachi ", Iaşi, 1992.
3. Popescu Şt. *Aplicaţii informatice în hidraulica sistemelor hidrotehnice.* Editura CERMI, Iaşi, 1999, ISBN 973-8000-11-4
4. Popescu Şt., Poiată T. *Determinarea caracteristicilor energo-economice echivalente ale unor instalaţii de pompare utilate cu agregate de pompare nereglabile.* În: Lucrările Conferinţei Naţionale de Termotehnică, Ediţia a VII-a, Vol.III, Braşov,1997, ISBN 973-97758-5-3.

MODELAREA FUNCȚIONARII UNEI INSTALAȚII DE POMPARE
CU HIDROFOR ÎN REGIMURI LENT VARIABILE

(Rezumat)

Se prezintă modelele conceptual şi matematic ce descriu funcționarea unei instalații de pompare prevăzute cu hidrofor, în regimurile cvasi-permanente şi tranzitorii lent-variabile. Această modelare, realizată în cadrul teoriei sistemelor, serveşte la determinarea principalilor indicatori de eficiență energo-economică a pompării apei şi la comanda pornirii/opririi agregatelor de pompare.